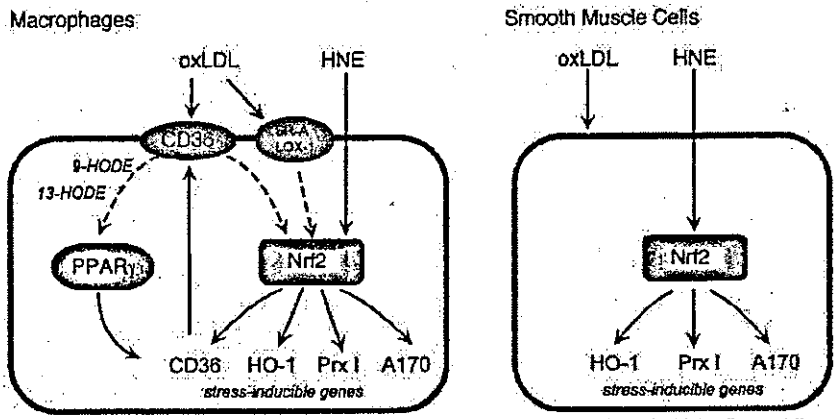

Figure 5. Nrf2-dependent activation of CD36 and antioxidant stress genes in murine peritoneal macrophages by oxidatively modified LDL (eg, moxLDL or oxLDL) or HNE. Activation of the Nrf2 pathway in macrophages leads to an upregulation of CD36 expression and uptake of oxidatively modified LDL. HNE, one of the end products of lipid peroxidation, induces rapid activation (2 to 5 hours) of Nrf2 and enhanced expression of HO-1, Prx I, and A170. Induction of antioxidant stress genes via Nrf2 affords protection of cells against the toxicity of oxLDLs. In murine aortic smooth muscle cells, expressing low levels of oxLDL scavenger receptors, oxidatively modified LDLs cause a negligible activation of Nrf2, whereas HNE can rapidly activate antioxidant gene expression via Nrf2. Dotted lines denote intracellular signaling cascades leading to the activation of PPAR-γ and/or Nrf2.

PPAR-γ directly,[11,34] whereas rapid activation of Nrf2 by HNE leads to CD36 gene expression in macrophages (Figures 3A and 3C), implicating Nrf2 as an important transcription factor in the upregulation of CD36 in oxidative stress. Third, as PPAR-γ activators 15d-PGJ_2 and rosiglitazone increased CD36 protein levels in both *nrf2*$^{+/+}$ and *nrf2*$^{-/-}$ macrophages (Figure 3D), this suggests that activation of PPAR-γ can occur in the absence of Nrf2.

HNE proved to be one of the most effective activators of Nrf2; however, we cannot exclude the possibility that other components of oxLDL may also have led to Nrf2 activation. Recent studies indicate that oxidized choline glycerophospholipid in oxLDL influences the binding of oxLDL to CD36.[36,37] Earlier studies from this group provided convincing evidence that lipid accumulation and foam cell formation were significantly reduced in *CD36*$^{-/-}$ mice.[38] Our preliminary studies with *CD36*$^{-/-}$ mice established that oxLDL and HNE induced activation of Nrf2 in murine macrophages is not dependent on CD36 (data not shown).

Kavanagh et al[39] reported that CD36 and PPAR-γ are differentially expressed in human monocytes in response to LDL oxidized to different degrees. Using oxLDL preparations similar to those in our study, this group established that moxLDL, but not oxLDL, enhanced DNA binding to PPAR-γ. Our experiments with *nrf2*$^{-/-}$ macrophages revealed that moxLDL still appears to increase, although not significantly, CD36 expression, whereas responses to oxLDL and HNE were abrogated (Figure 3C). We believe that HNE selectively activates Nrf2, resulting in a PPAR-γ–independent expression of CD36 in macrophages. In this context, HNE has been detected in rabbit and human atherosclerotic lesions,[40,41] and Napoli et al[42] reported that a large percentage of all fetal aortic atherogenic sites contained malondialdehyde-lysine and HNE-lysine epitopes.

Our findings in *nrf2*$^{+/+}$ macrophages indicate that moxLDL and oxLDL selectively upregulate CD36 mRNA expression (Figure 4A) but not the scavenger receptors LOX-1 or SR-A (data not shown). In contrast, in *nrf2*$^{-/-}$ macrophages oxLDLs and HNE fail to significantly increase CD36 levels (Figure 3C). We found multiple ARE-like sequences in the promotor region of murine CD36-encoding gene (GenBank accession No. AF434766) and further studies are required to identify the functional Nrf2-interacting ARE in this promotor region. A recent study indicates that AREs play a direct role in mediating the induction of glutathione synthesis by oxLDL, suggesting a role of Nrf2 in this response.[43] The lack of induction of CD36 in *nrf2*$^{-/-}$ macrophages was associated with a reduced accumulation of cholesterol (Figures 4B and 4C), indicating that the Nrf2 signaling pathway plays a key role in mediating oxLDL uptake via CD36. Although there are limited reports that human cultured aortic SMCs express CD36,[44–46] we could not detect CD36 expression in SMCs cultured from either *nrf2*$^{+/+}$ and *nrf2*$^{-/-}$ mice (data not shown). These differences in CD36 expression may be important for comparisons of human and murine models of atherosclerosis.

Our study provides the first evidence that Nrf2, in addition to coordinating cellular defenses against electrophilic agents and reactive oxygen species, also plays an essential role in regulating CD36 expression. Figure 5 summarizes our experimental findings, and highlights that in murine macrophages oxLDLs and HNE lead to a rapid nuclear accumulation of Nrf2 and subsequent induction of CD36 and the stress proteins A170, HO-1, and Prx I. In murine SMCs, oxLDLs fail to induce nuclear translocation of Nrf2 and gene activation of CD36 and stress proteins most likely due to the fact that murine SMCs express low levels of scavenger receptors. In *nrf2*$^{-/-}$ macrophages, oxLDLs could still signal via PPAR-γ, whereas the Nfr2-dependent induction of antioxidant stress proteins is markedly attenuated. The recent report that PPAR-γ inhibits Nrf2-induced expression of the gene encoding thromboxane synthase in macrophages,[47] suggests that the transcriptional regulators PPAR-γ and Nrf2 may interact functionally to modulate CD36 gene expression.

Future studies in vivo, using wild-type and Nrf2-deficient mice, should enable us to determine whether Nrf2 is expressed in atherosclerotic lesions, and whether this transcription factor modulates the progression of foam cell formation and atherosclerosis. Because Nrf2 has been implicated as a regulator of HO-1 expression and HO-1 mRNA and protein levels are increased in human atherosclerotic lesions,[29] it seems likely that Nrf2 plays a role in atherogenesis. Identi-

fying the intracellular signaling pathways modulating Nrf2 and PPAR-γ will provide important insights into their role in regulating vascular gene expression[48] and may provide a basis for the design of therapeutic strategies to treat atherosclerosis.

Acknowledgments

This work was supported by the Japan Society for the Promotion of Science, University of Tsukuba Research Projects, and a Wellcome Trust Short-Term Collaborative Travel Grant (T. I., G.E.M.). We thank Dr S. Taketani (Kansai Medical University, Moriguchi, Osaka, Japan) for providing the anti–HO-1 antibody, Dr Maria Febbraio (Medical College of Cornell University, Ithaca, NY) for providing the *CD36*-deficient mice, and Dr David Greaves, Dr Richard Siow, and Prof Jeremy Pearson for their helpful discussion of this work.

References

1. Ross R. Atherosclerosis: an inflammatory disease. *N Engl J Med.* 1999; 340:115–126.
2. Steinberg D. Low density lipoprotein oxidation and its pathobiological significance. *J Biol Chem.* 1997;272:20963–20966.
3. Greaves DR, Gough PJ, Gordon S. Recent progress in defining the role of scavenger receptors in lipid transport, atherosclerosis and host defence. *Curr Opin Lipidol.* 1998;9:425–432.
4. de Villiers DR, Gough PJ, Gordon S. Macrophage scavenger receptors and foam cell formation. *J Leukoc Biol.* 1999;66:740–746.
5. Steinbrecher UP. Receptors for oxidized low density lipoprotein. *Biochim Biophys Acta.* 1999;1436:279–298.
6. Esterbauer H, Gebicki J, Puhl H, Jurgens G. The role of lipid peroxidation and antioxidants in oxidative modification of LDL. *Free Radic Biol Med.* 1992;13:341–390.
7. Frostegard J, Wu R, Giscombe R, Holm G, Lefvert AK, Nilsson J. Induction of T-cell activation by oxidized low density lipoprotein. *Arterioscler Thromb.* 1992;12:461–467.
8. Cushing SD, Berliner JA, Valente AJ, Territo MC, Navab M, Parhami F, Gerrity R, Schwartz CJ, Fogelman AM. Minimally modified low density lipoprotein induces monocyte chemotactic protein 1 in human endothelial cells and smooth muscle cells. *Proc Natl Acad Sci USA.* 1990;87: 5134–5138.
9. Yamaguchi M, Sato H, Bannai S. Induction of stress proteins in mouse peritoneal macrophages by oxidized low-density lipoprotein. *Biochem Biophys Res Commun.* 1993;193:1198–1201.
10. Siow RC, Sato H, Leake DS, Pearson JD, Bannai S, Mann GE. Vitamin C protects human arterial smooth muscle cells against atherogenic lipoproteins: effects of antioxidant vitamins C and E on oxidized LDL-induced adaptive increases in cystine transport and glutathione. *Arterioscler Thromb Vasc Biol.* 1998;18:1662–1670.
11. Nagy L, Tontonoz P, Alvarez JGA, Chen H, Evans M. Oxidized LDL regulates macrophage gene expression through ligand activation of PPARγ. *Cell.* 1998;93:229–240.
12. Ricote M, Li AC, Willson TM, Kelly CJ, Glass CK. The peroxisome proliferator-activated receptor-γ is a negative regulator of macrophage activation. *Nature.* 1998;391:79–82.
13. Jiang C, Ting AAT, Seed B. PPAR-γ agonists inhibit production of monocyte inflammatory cytokines. *Nature.* 1998;391:82–86.
14. Moore KJ, Rosen ED, Fitzgerald KL, Randow F, Andersson LP, Altshuler D, Milstone DS, Mortensen RM, Spiegelman BM, Freeman MW. The role of PPAR-γ in macrophage differentiation and cholesterol uptake. *Nat Med.* 2001;7:41–47.
15. Chawla A, Barak Y, Nagy L, Liao D, Tontonoz P, Evans M. PPAR-γ dependent and independent effects on macrophage-gene expression in lipid metabolism and inflammation. *Nat Med.* 2001;7:48–52.
16. Itoh K, Chiba T, Takahashi S, Ishii T, Igarashi K, Katoh Y, Oyake T, Hayashi N, Satoh K, Hatayama I, Yamamoto M, Nabeshima Y. An Nrf2/small Maf heterodimer mediates the induction of phase II detoxifying enzyme genes through antioxidant response elements. *Biochem Biophys Res Commun.* 1997;236:313–322.
17. Ramos-Gomez M, Kwak MK, Dolan PM, Itoh K, Yamamoto M, Talalay P, Kensler TW. Sensitivity to carcinogenesis is increased and chemoprotective efficacy of enzyme inducers is lost in nrf2 transcription factor-deficient mice. *Proc Natl Acad Sci USA.* 2001;98:3410–3415.
18. Kwak MK, Itoh K, Yamamoto M, Sutter TR, Kensler TW. Role of transcription factor Nrf2 in the induction of hepatic phase 2 and antioxidative enzymes in vivo by the cancer chemoprotective agent, 3*H*-1,2-dimethiole-3-thione. *Mol Med.* 2001;7:135–145.
19. Cho HY, Jedlicka AE, Reddy SP, Kensler TW, Yamamoto M, Zhang LY, Kleeberger SR. Role of Nrf2 in protection against hyperoxic lung injury in mice. *Am J Respir Cell Mol Biol.* 2002;26:175–182.
20. Ishii T, Itoh K, Takahashi S, Sato H, Yanagawa T, Katoh Y, Bannai S, Yamamoto M. Transcription factor Nrf2 coordinately regulates a group of oxidative stress-inducible genes in macrophages. *J Biol Chem.* 2000;275: 16023–16029.
21. Itoh K, Wakabayashi N, Katoh Y, Ishii T, Igarashi K, Engel JD, Yamamoto M. Keap1 represses nuclear activation of antioxidant responsive elements by Nrf2 through binding to the amino-terminal Neh2 domain. *Genes Dev.* 1999;13:76–86.
22. Itoh K, Wakabayashi N, Katoh Y, Ishii T, O'Connor T, Yamamoto M. Keap1 regulates both cytoplasmic-nuclear shuttling and degradation of Nrf2 in response to electrophiles. *Genes Cells.* 2003;8:379–391.
23. Siow RCM, Ishii T, Sato H, Taketani S, Leak DS, Sweiry JH, Pearson JD, Bannai S, Mann GE. Induction of the antioxidant stress proteins heme oxygenase-1 and MSP23 by stress agents and oxidized LDL in cultured vascular smooth muscle cells. *FEBS Lett.* 1995;368:239–242.
24. Wang LJ, Lee TS, Lee FY, Pai RC, Chau LY. Expression of heme oxygenase-1 in atherosclerotic lesions. *Am J Pathol.* 1998;152:711–720.
25. Lee TS, Chau LY. Heme oxygenase-1 mediates the anti-inflammatory effect of interleukin-10 in mice. *Nat Med.* 2002;8:240–246.
26. Kang SW, Chae HZ, Seo MS, Kim K, Baines IC, Rhee SG. Mammalian peroxiredoxin isoforms can reduce hydrogen peroxide generated in response to growth factors and tumor necrosis factor-α. *J Biol Chem.* 1994;91:7022–7026.
27. Jin D-Y, Chae HZ, Rhee SG, Jeang K-T. Regulatory role for a novel human thioredoxin peroxidase in NF-κB activation. *J Biol Chem.* 1997; 272:30952–30961.
28. Leonarduzzi G, Arkan MC, Basaga H, Chiarpotto E, Sevanian, Poli G. Lipid oxidation products in cell signaling. *Free Radic Biol Med.* 2000; 1370–1378.
29. Han J, Hajjar DP, Febbraio M, Nicholson AC. Native and modified low density lipoproteins increase the functional expression of the macrophage class B scavenger receptor, CD36. *J Biol Chem.* 1997;272:21654–21659.
30. Yoshida H, Quehenberger O, Kondratenko N, Green S, Steinberg D. Minimally oxidized low-density lipoprotein increases expression of scavenger receptor A, CD36, and macrosialin in resident mouse peritoneal macrophages. *Arterioscler Thromb Vasc Biol.* 1998;18:794–802.
31. Kawane T, Hou JQ, Sato H, Sugita Y, Bannai S, Ishii T. Induction of metalloelastase mRNA in murine peritoneal macrophages by diethylmaleate. *Biochim Biophys Acta.* 1999;1427:155–160.
32. Glass CK. Potential roles of the peroxisome proliferator-activated receptor-γ in macrophage biology and atherosclerosis. *J Endocrinol.* 2001;169:461–464.
33. Klappacher GW, Glass CK. Roles of peroxisome proliferator-activated receptor γ in lipid homeostasis and inflammatory responses of macrophages. *Curr Opinion Lipdol.* 2002;13:305–312.
34. Tontonoz P, Nagy L, Alvarez JGA, Thomazy VA, Evans RM. PPARγ promotes monocyte/macrophage differentiation and uptake of oxidized LDL. *Cell.* 1998;93:241–252.
35. Ricote M, Huang J, Fajas L, Li A, Welch J, Najib J, Witztum JL, Auwerx J, Palinski W, Glass CK. Expression of the peroxisome proliferator-activated receptor γ (PPAR-γ) in human atherosclerosis and regulation in macrophages by colony stimulating factors and oxidized low density lipoprotein. *Proc Natl Acad Sci USA.* 1998;95:7614–7619.
36. Podrez EA, Poliakov E, Shen Z, Zhang R, Deng Y, Sun M, Finton PJ, Shan L, Febbraio M, Hajjar DP, Silverstein RL, Hoff HF, Salomon RG, Hazen SL. A novel family of atherogenic oxidized phospholipids promotes macrophage foam cell formation via the scavenger receptor CD36 and is enriched in atherosclerotic lesions. *J Biol Chem.* 2002;277:38517–38523.
37. Podrez EA, Hoppe G, O'Neil J, Hoff HF. Phospholipids in oxidized LDL not adducted to apoB are recognized by the CD36 scavenger receptor. *Free Radic Biol Med.* 2003;34:356–364.
38. Febbraio M, Podrez EA, Smith JD, Hajjar DP, Hazen SL, Hoff HF, Sharma K, and Silverstein RL. Targeted disruption of the class B scavenger receptor CD36 protects against atherosclerotic lesion development in mice. *J Clin Invest.* 2000;105:1049–1056.
39. Kavanagh IC, Symes CE, Renaudin P, Nova E, Mesa MD, Boukouvalas G, Leake DS, Yaqoob P. Degree of oxidation of low density lipoprotein

affects expression of CD36 and PPARγ, but not cytokine production, by human monocyte-macrophages. *Atherosclerosis.* 2003;2:271–282.
40. Brasen JH, Hakkinen T, Malle E, Beisiegel U, Yla-Herttula S. Patterns of oxidized epitopes, but not NFκB expression, change during atherogenesis in WHHL rabbits. *Atherosclerosis.* 2003;166:13–21.
41. Jurgens G, Chen Q, Esterbauer H, Mair S, Ledinski G, Dinges HP. Immunostaining of human autopsy aortas with antibodies to modified apolipoprotein B apoprotein(a). *Arterioscler Thromb.* 1993;13:1689–1699.
42. Napoli C, D'Armiento FP, Mancini FP, Postiglione A, Witzum JL, Palumbo G, Palinski W. Fatty streak formation occurs in human fetal aortas and is greatly enhanced by maternal hypercholesterolemia. Intimal accumulation of low density lipoprotein and its oxidation products precede monocyte recruitment into early atherosclerotic lesions. *J Clin Invest.* 1997;11:2680–2690.
43. Bea F, Hudson FN, Chait A, Kavanagh TJ, Rosenfeld ME. Induction of glutathione synthesis in macrophages by oxidized low-density lipoproteins is mediated by consensus antioxidant response elements. *Circ Res.* 2003;92:386–393.
44. Ricciarelli R, Zingg JM, Azzi A. Vitamin E reduces the uptake of oxidized LDL by inhibiting CD36 scavenger receptor expression in cultured aortic smooth muscle cells. *Circulation.* 2000;102:82–87.
45. Matsumoto K, Hirano K, Nozaki S, Takamoto, Nishida M, Malagawa-Toyama Y, Janabi MY, Ohya T, Yamashita S, Matsuzawa Y. Expression of macrophage (Mϕ) scavenger receptor, CD36, in cultured human aortic smooth muscle cells in association with expression of peroxisome proliferator activated receptor-γ, which regulates gain of Mϕ-like phenotype in vitro and its implications in atherogenesis. *Arterioscler Thromb Vasc Biol.* 2000;20:1027–1032.
46. Bishop-Bailey D, Hla T, Warner TD. Intimal smooth muscle cells as a target for peroxisome proliferator-activated receptor-γ ligand therapy. *Circ Res.* 2002;91:210–217.
47. Ikeda Y, Sugawara A, Taniyama Y, Urano A, Igarashi K, Arima S, Ito S, Takeuchi K. Suppression of rat thromboxane synthase gene transcription by peroxisome proliferator-activated receptor γ in macrophages via an interaction with Nrf2. *J Biol Chem.* 2000;275:33142–33150.
48. Kunsch C, Medford RM. Oxidative stress as a regulator of gene expression in the vasculature. *Circ Res.* 1999;85:753–765.

Protection against electrophile and oxidant stress by induction of the phase 2 response: Fate of cysteines of the Keap1 sensor modified by inducers

Nobunao Wakabayashi*†‡, Albena T. Dinkova-Kostova*, W. David Holtzclaw*, Moon-Il Kang‡, Akira Kobayashi‡, Masayuki Yamamoto‡, Thomas W. Kensler*†, and Paul Talalay*§

*The Lewis B. and Dorothy Cullman Cancer Chemoprotection Center, Department of Pharmacology and Molecular Sciences, School of Medicine, and †Department of Environmental Health Sciences, Bloomberg School of Public Health, The Johns Hopkins University, Baltimore, MD 21205; and ‡Center for Tsukuba Advanced Research Alliance and Japan Science and Technology Agency/Exploratory Research for Advanced Technology Environmental Response Project, University of Tsukuba, 1-1-1 Tennoudai, Tsukuba 305-8575, Japan

Contributed by Paul Talalay, December 12, 2003

Induction of a family of phase 2 genes encoding for proteins that protect against the damage of electrophiles and reactive oxygen intermediates is potentially a major strategy for reducing the risk of cancer and chronic degenerative diseases. Many phase 2 genes are regulated by upstream antioxidant response elements (ARE) that are targets of the leucine zipper transcription factor Nrf2. Under basal conditions, Nrf2 resides mainly in the cytoplasm bound to its cysteine-rich, Kelch domain-containing partner Keap1, which is itself anchored to the actin cytoskeleton and represses Nrf2 activity. Inducers disrupt the Keap1-Nrf2 complex by modifying two (C273 and C288) of the 25 cysteine residues of Keap1. The critical role of C273 and C288 was established by (*i*) their high reactivity when purified recombinant Keap1 was treated with dexamethasone mesylate and the dexamethasone-modified tryptic peptides were analyzed by mass spectrometry, and (*ii*) transfection of *keap1* and *nrf2* gene-deficient mouse embryonic fibroblasts with constructs expressing cysteine to alanine mutants of Keap1, and measurement of the ability of cotransfected Nrf2 to repress an ARE-luciferase reporter. Reaction of Keap1 with inducers results in formation of intermolecular disulfide bridges, probably between C273 of one Keap1 molecule and C288 of a second. Evidence for formation of such dimers was obtained by 2D PAGE of extracts of cells treated with inducers, and by the demonstration that whereas C273A and C288A mutants of Keap1 alone could not repress Nrf2 activation of the ARE-luciferase reporter, an equal mixture of these mutant constructs restored repressor activity.

This paper describes the molecular mechanisms that control expression of phase 2 genes, which play central roles in protecting aerobic life against the relentless stresses imposed by electrophiles and reactive oxygen intermediates: the principal causes of many chronic diseases, including cancer. Many phase 2 proteins are enzymes that are highly inducible by transcriptional activation, and exert versatile, long-acting, and often catalytic protection against electrophile and oxidative damage. Phase 2 proteins comprise not only the "classical" phase 2 xenobiotic-metabolizing enzymes such as glutathione transferases and UDP-glucuronosyltransferases, which conjugate xenobiotics with endogenous ligands, but include also NAD(P)H:quinone reductase (NQO1) (EC 1.6.99.2), epoxide hydrolase, heme oxygenase 1, ferritin, γ-glutamylcysteine ligase, glutathione reductase, aldehyde dehydrogenase, dihydrodiol dehydrogenase, leukotriene B_4 dehydrogenase, and glutathione *S*-conjugate efflux pumps (reviewed in refs. 1 and 2).

Much evidence supports the notion that induction of the phase 2 response is an efficient strategy for reducing the risk of a variety of diseases (for reviews, see refs. 2–4). For example: (*i*) mice in which the phase 2 response has been silenced (*nrf2* gene knockouts) have low and uninducible phase 2 enzymes, are much more susceptible to carcinogens and the toxicity of oxygen and electrophiles and, unlike cognate wild-type mice, cannot be protected by inducers (2, 5–7). (*ii*) Targeted disruption of two phase 2 enzymes in mice (glutathione transferase π and NQO1) increased incidence of skin tumors evoked by polycyclic hydrocarbons (8, 9). (*iii*) Bioassays of phase 2 inducer potency, based on quantifying NQO1 activity in murine hepatoma cells, resulted in the isolation of several potent anticarcinogenic inducers, including sulforaphane from broccoli, and have also guided the synthesis of potent inducers (for review, see ref. 2). (*iv*) Human populations polymorphic for certain phase 2 enzymes are more susceptible to toxicity and carcinogenesis (10–13). (*v*) Administration of the phase 2 inducer oltipraz to individuals at very high risk of developing primary hepatocellular carcinoma, because of heavy dietary intakes of aflatoxin B_1, substantially increased excretion of phase 2 metabolites of aflatoxin, a biomarker for carcinogen load (14).

Inducers of phase 2 genes belong to nine structurally highly diversified chemical classes (15, 16), and share only a few common properties (17): (*i*) all are chemically reactive; (*ii*) nearly all are electrophiles; (*iii*) most are substrates for glutathione transferases; and (*iv*) all can modify sulfhydryl groups by alkylation, oxidation, or reduction. Recognition of these properties suggested that cells contain primary sensor(s) equipped with highly reactive cysteine residues that are recognized and chemically modified by inducers, thereby initiating the enhanced transcription of phase 2 genes. We have recently obtained evidence that Kelch-like ECH-associated protein 1 (Keap1) is probably this regulatory sensor (18), a conclusion that is strongly supported by the accompanying paper (19), and other very recent studies (20, 21).

Phase 2 genes are regulated by 5′ upstream regulatory sequences which have been designated as antioxidant response elements (ARE) (22, 23). Nrf2, a member of the NF-E2 family of nuclear basic leucine zipper transcription factors, binds to the ARE, and accelerates transcription of the cognate genes (24–26). Under basal conditions, Keap1, a recently identified protein associated with the actin cytoskeleton, binds very tightly to Nrf2, anchors this transcription factor in the cytoplasm, and targets it for ubiquitination and proteasome degradation, thereby repressing the ability of Nrf2 to induce phase 2 genes (27–32). Inducers disrupt the Keap1-Nrf2 complex, allowing Nrf2 to translocate to the nucleus where, in heterodimeric combinations with other

Abbreviations: ARE, antioxidant response element; NQO1, nicotinamide quinone oxidoreductase 1, NAD(P)H:quinone acceptor oxidoreductase 1; KONO, *nrf2/keap1* double knockout; Dex-mes, dexamethasone 21-mesylate; Keap1, Kelch-like ECH-associated protein 1; IVR, intervening region of Keap1; C257A, C257 replaced by alanine; C257A–C297A, all cysteine residues from C257 to C297 replaced by alanine.

§To whom correspondence should be addressed at: Department of Pharmacology and Molecular Sciences, The Johns Hopkins University School of Medicine, 725 North Wolfe Street, Baltimore, MD 21205. E-mail: ptalalay@jhmi.edu.

www.pnas.org/cgi/doi/10.1073/pnas.0307301101

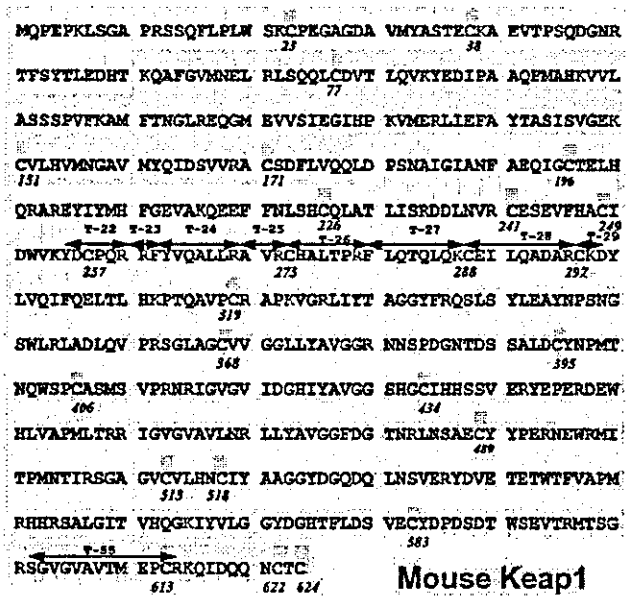

Fig. 1. Amino acid sequence of the five domains of Keap1: (*i*) N-terminal region (NTR, amino acids 1–60: two cysteines, blue). (*ii*) BTB (Broad complex, Tramtrack, Bric-a-Brac; amino acids 61–179: three cysteines, pink), an evolutionarily conserved protein–protein interaction motif that often dimerizes with other BTB domains (33). (*iii*) IVR (amino acids 180–314: eight cysteines, yellow). (*iv*) Double glycine (DGR, amino acids 315–598: nine cysteines, gray) comprising six Kelch motifs (amino acids 315–359, 361–410, 412–457, 459–504, 506–551, and 553–598). Repeated Kelch motifs give rise to a β-propeller structure with multiple protein-binding sites (34). The DGR of Keap1 binds tightly to the Neh2 segment (the 100 N-terminal amino acids) of Nrf2 (24, 27), and is also the region involved in anchoring Keap1 to the actin cytoskeleton (19). (*v*) C-terminal region (CTR, amino acids 599–624: three cysteines, green). The 25 cysteine residues are highlighted in bright yellow, the 39 arginine residues are blue, and the 17 lysine residues are red. The tryptic peptides labeled with dexamethasone (T-22, T-26, T-28, T-29, and T-55) are designated. The matrix-assisted laser desorption ionization/time-of-flight mass spectral analyses of all 57 tryptic peptides, including the 19 peptides that contain cysteine residues are recorded in Table 1 (see *Supporting Text*).

basic leucine zipper proteins, it binds to AREs of phase 2 genes and accelerates their transcription.

The 624 amino acids of murine Keap1 include 25 cysteines and comprise five domains (Fig. 1). Because all cysteine residues are conserved, identification of those critical for induction presented special problems. Consequently, we resorted to the strategy of first identifying the most reactive cysteines by chemical modification with dexamethasone 21-mesylate (Dex-mes), an inducer that reacts irreversibly with thiols, and second, examining whether mutations of these residues alter the ability of Keap1 to repress Nrf2 function. Four cysteines [C257, C273, C288, and C297, all located in the intervening region (IVR) domain] of purified recombinant Keap1 were most reactive with Dex-mes (18), suggesting strongly that Keap1 is the molecular sensor for inducers. We now establish the critical functional role of these reactive cysteine thiols of Keap1 in signaling induction, by further analysis of the Dex-mes-modified tryptic peptides of Keap1, and by introducing systematic mutations of these cysteine residues.

Experimental Procedures

Constructs. Each Cys to Ala mutant of Keap1 was produced by PCR and standard recombination techniques. Construct authenticity was confirmed by sequencing. pcDNA3 or pET vectors were used for mammalian or bacterial cell expression, respectively, as described (18). All primers and PCR conditions used for genotyping and for the preparation of the constructs used in this study are listed in *Supporting Text*, which is published as supporting information on the PNAS web site.

Production of *keap1*(−/−) and Combined *keap1*(−/−)::*nrf2*(−/−) Mouse Embryonic Fibroblasts. Fibroblasts were isolated from 13.5-day-old embryos of *keap1*(−/−) and *keap1*(−/−)::*nrf2*(−/−) mice and used to establish stable lines by standard procedures (35). Cells were maintained in Iscove's modified Eagle's medium, supplemented with 10% heat-inactivated FBS, at 37°C and 5% CO_2.

Functional Reporter Assay. Transient reporter assays were performed by standard transfection methods using 2×10^5 *keap*(−/−)::*nrf2*(−/−) mouse embryonic fibroblast (MEF) cells (K0N0) in 60-mm diameter dishes. Each construct of plasmid [2 μg of reporter gene pNQO1AREluc, 2 μg of pRLTK-normalizing vector, 8 μg of pCMVmNrf2, and various amounts (see Fig. 4) of each Keap1 expression vector, with total DNA adjusted to 2 μg with pcDNA3] was introduced into K0N0 MEF cells by the calcium phosphate co-precipitation method. Two micrograms of pRLTK plasmid bearing the *Renilla* luciferase gene under the control of the HSV-tk promoter/enhancer were included in each transfection and used for normalization. Cells were harvested 24 h after transfection and luciferase activities were measured according to the manufacturer's instructions (Promega). Relative luciferase activity was obtained from six independent transfection experiments and is shown ±SEM in each figure.

Nonreducing-Reducing 2D SDS/PAGE. HEK293 cells (5×10^5 per 60-mm dish) were transfected with 20 μg of pEFmKeap1. After transfection (48 h), the medium was exchanged with serum-free medium containing 250 μM DTT, and cells were incubated for 3 h. After extensive washing with PBS (5×), cells were exposed to an inducer or vehicle and incubated in medium at 37°C, 5% CO_2 for 6 h, and finally harvested with 150 μl of RIPA buffer (10 mM Tris·HCl, pH 7.5/1% Nonidet P-40/0.1% Na-deoxycholate/0.1% SDS/150 mM NaCl/1 mM EDTA). Samples were boiled with DTT-free SDS buffer, and 25 μg of protein were subjected to nonreducing disk-gel (2-mm diameter disk) SDS/PAGE. Gels were ejected and reduced with 1× SDS buffer including 5% 2-mercaptoethanol at room temperature for 1 h, with one buffer change. Disk gels were inserted into the well of a second SDS/PAGE and subjected to electrophoresis.

Immunoblotting. Keap1 was detected by using rabbit anti-mKeap1 polyclonal antibody (25, 28). For normalizing cell number, nuclear Lamin B was detected from the same extracts with goat anti-Lamin B antibody (Santa Cruz Biotechnology). For normalizing transfection efficiency, Bsd-GFP protein, encoded from the same plasmid as Keap1, was detected by goat anti-GFP antibody (Santa Cruz Biotechnology). Membranes were blocked and treated with primary antibody followed by reaction with the appropriate secondary antibodies conjugated to horseradish peroxidase (Zymed, Bio-Rad). Immune complexes were visualized with enhanced chemiluminescence (Amersham Pharmacia).

Results and Discussion

Identification of the Most Reactive Cysteine Residues of Keap1 and Their Importance for Inducer and Nrf2-Binding Activity. In further validation that Keap1 contains highly reactive cysteine thiols that sense inducers (18), we carried out additional experiments with Dex-mes, an inducer which alkylates thiols irreversibly, and increases their masses substantially (374.19 atomic mass units). Homogeneous recombinant Keap1 (600 pmol) was incubated with a modest excess of Dex-mes (6 nmol) at 25°C and pH 8.0,

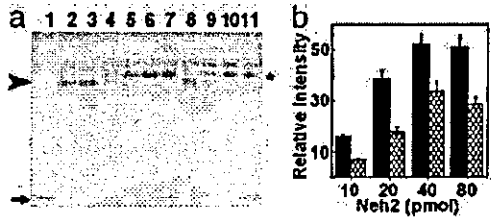

Fig. 2. Comparison of binding of wild-type and mutant (C257A–C297A) Keap1 to the Neh2 domain of Nrf2. (*a*) Native gel electrophoresis showing complex between Keap1 (100 pmol) and the Neh2 domain of Nrf2 (10, 20, 40, and 80 pmol, lanes 4–7 and 8–11, respectively). Lane 1, Neh2; lane 2, wild-type Keap1; lane 3, mutant Keap1. Lanes 4–7 show progressively increasing quantities of complex between wild-type Keap1 and Neh2; lanes 8–11 show lower quantities of complex formation between mutant Keap1 and Neh2. Arrowhead, arrow, and asterisk show Keap1, Neh2, and Neh2-Keap1 or mutant Keap1 complex bands, respectively. (*b*) Densitometric quantification of the intensities of bands of complexes between Neh2 and wild-type Keap1 (black bars) and mutant Keap1 (hatched bars).

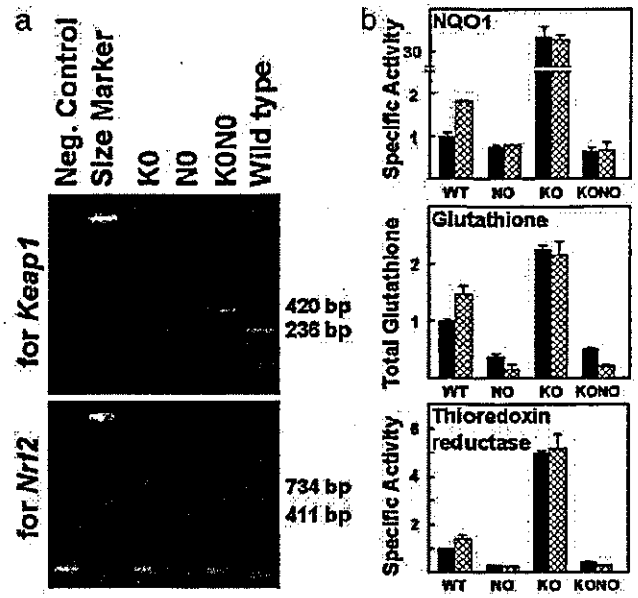

Fig. 3. Genotyping and levels of expression of phase 2 gene products in established lines of embryonic fibroblasts obtained from mice in which the *keap1* (K0), *nrf 2* (N0), or both genes (K0N0) were disrupted. (*a*) Electrophoresis of the PCR products derived from *keap1* wild-type (236 bp) and mutant (420 bp) alleles, and *nrf2* wild-type (734 bp) and mutant (411 bp) alleles. (*b*) Comparison (normalized to wild-type controls) of the specific activities of NQO1 and thioredoxin reductase, and concentration of glutathione in cell-free extracts of the three mutant and wild-type mouse embryonic fibroblasts. Black bars, cells untreated with inducers; hatched bars, cells exposed for 24 h to 1.5 μM sulforaphane.

for 2 h. Excess Dex-mes was removed by gel filtration, and the denatured protein was treated with *N*-ethylmaleimide to alkylate unreacted thiols. Tryptic peptides were separated by reversed-phase HPLC, fractions were analyzed by matrix-assisted laser desorption ionization/time-of-flight (MALDI-TOF) MS. The 57 tryptic peptides were designated T-1 to T-57. All of the predicted 19 cysteine-containing tryptic peptides were recovered in the fractions (either as single peptides or as incompletely cleaved di- or tripeptides). Their masses agreed within 0.5 atomic mass units with calculated values (see Table 1, which is published as supporting information on the PNAS web site). Peptides containing C257 (T-22), C273 (T-25 to T-28), C288 (T-28), C297 (T-29), and C613 (T-55) (see Fig. 1) were found to have mass increases corresponding to the covalent addition of the steroid. All other cysteine-containing peptides showed mass increases of 125.05 atomic mass units (for each cysteine residue), indicating alkylation by *N*-ethylmaleimide. Thus, in agreement with our earlier findings, C257, C273, C288, and C297, all located in the IVR domain, as well as C613, are the most reactive cysteine residues of native Keap1 *in vitro* (18).

The reproducible labeling of 4 specific cysteines of Keap1 prompted us to examine the properties of recombinant Keap1 in which these cysteine residues were replaced by alanine. The mutant protein (C257A–C297A) was overexpressed in *E. coli* and purified to homogeneity by our procedure used to purify wild-type Keap1 (18). Both wild-type and mutant proteins migrated identically on native and SDS/PAGE (molecular weight ≈ 65,000).

Comparison of rates of binding of [^{3}H]Dex-mes and sulforaphane to purified wild-type and mutant (C257A–C297A) Keap1, measured by tritium incorporation and dithiocarbamate formation, respectively, revealed that the reaction rates of the mutant were ≈50% slower, confirming that the modified cysteines were indeed the most reactive in the native protein.

We next examined whether the four most reactive cysteine residues of Keap1 influenced binding to Nrf2. Incubation of Keap1 with the Neh2 (Keap1 binding) domain of Nrf2 under reducing conditions led to formation of a complex that can be detected by native PAGE (Fig. 2*a*). At a constant Keap1 concentration, the intensity of the band corresponding to the complex increases with increasing amounts of Neh2, reaching saturation at a ratio of Keap1 to Neh2 of ≈2:1. Both wild-type and mutant Keap1 can form complexes with Neh2, but the mutant protein has ≈50% lower affinity for Neh2 based on band density (Fig. 2*b*).

Two separate lines of evidence, rates of reaction with inducers and binding to the Neh2 domain, indicate that the mutant Keap1 in which four specific cysteine residues in the IVR (C257A–C297A) were mutated not only reacted markedly more slowly with inducers, but also displayed a parallel decrease in affinity for the Neh2 domain of Nrf2. This is powerful evidence for the importance of these cysteines of Keap1 for repression of Nrf2.

Preparation and Properties of Mouse Embryonic Fibroblasts in Which *keap1*, *nrf2*, or both Genes Have Been Disrupted. Further understanding of the regulatory functions of Keap1 and its mutants by transfection analyses of whole cells required cell lines in which interference from endogenous Keap1 and Nrf2 was eliminated. Consequently, we established cell lines from primary cultures of embryo fibroblasts of wild-type, *nrf2*-knockout (N0), *keap1*-knockout (K0), and K0N0 mice (36) (Fig. 3*a*). Wild-type cells have readily detectable basal levels of NQO1, glutathione, and thioredoxin reductase, which were elevated upon exposure to 1.5 μM sulforaphane (Fig. 3*b*). N0 and K0N0 cells have lower and essentially uninducible levels of these components. Moreover, the already lower levels of glutathione were further reduced by >50% upon treatment with sulforaphane, most likely because of direct conjugation with reduced glutathione (37). In sharp contrast, K0 cells have much higher basal levels compared to their wild-type counterparts, and essentially no induction was observed upon exposure to sulforaphane. These findings confirm the critical role of the Keap1/Nrf2 system for both basal and inducible expression of these phase 2 responses, and are consistent with the proposed repression of Nrf2 by Keap1.

Repression by Keap1 of ARE- and Nrf2-Dependent Gene Expression: Mutations of Cysteine Residues of Keap1. Effects of specific cysteine to alanine mutations on the ability of Keap1 to repress Nrf2 *in*

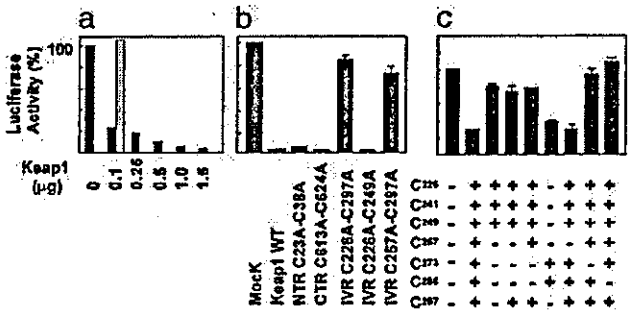

Fig. 4. Repression of the intensity of luciferase luminescence of ARE-luciferase in K0N0 mouse embryonic fibroblasts by wild-type Keap1 and its cysteine mutants. All cells were transfected with the ARE-luciferase (2 μg) and the Nrf2 (8 μg) constructs. (*a*) Repression of luminescence as a function of amount of wild-type Keap1 (black bars) and its reversal by exposure to 2 μM sulforaphane (gray bar). (*b*) Repression of luminescence by wild-type (WT) Keap1 (2 μg) and equivalent quantities of the following mutants: NTR (C23A and C38A); CTR (C613A, C622A, and C624A); IVR C226A–C297A (C226A, C241A, C249A, C257A, C273A, C288A, and C297A); IVR C226A–C249A (C226A, C241A, and C249A); and IVR C257A–C297A (C257A, C273A, C288A, and C297A). (*c*) Repressive activity of single or multiple cysteine mutants of Keap1 with 100 ng of each expression vector. The structures of the mutants are designated: + for cysteine, − for alanine. The structure of each wild-type and mutant Keap1 is shown below the bar indicating its repressor activity. Repressor activity is abrogated if C273 or C288, or both, are mutated to alanine.

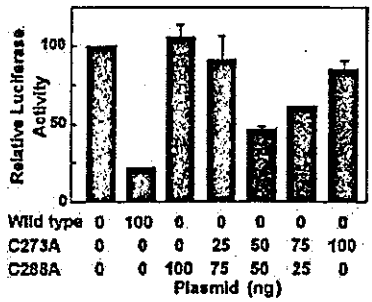

Fig. 5. Repression of the intensity of luciferase luminescence of ARE-luciferase in K0N0 mouse embryo fibroblasts by wild-type Keap1 and its C273A and C288A mutants. All cells were transfected with the ARE-luciferase (2 μg) and the Nrf2 (8 μg) constructs. The luminescence observed in the absence of Keap1 is expressed as 100 units. Addition of 100 ng of wild-type Keap1 plasmid reduced the luminescence to ~20%. The plasmids (100 ng) coding for C273A or C288A showed little, if any, repression of the fluorescence, whereas mixtures of these plasmids restored the repressor activity. A mixture of 50 ng of each plasmid repressed ~40% of the luminescence of the system.

vivo were examined by transient transfection experiments in mouse embryonic fibroblasts from *keap1/nrf2* double knockout animals (K0N0). K0N0 cells were transiently transfected with controlled quantities of three vectors: (*i*) an Nrf2 expression vector (pCMVmNrf2); (*ii*) a vector that expresses either wild-type or mutants of Keap1; and (*iii*) a luciferase reporter vector controlled by the ARE of NQO1 (pNQO1AREluc) (38). The effect of mutating cysteine residues of Keap1 on the luciferase activity provided a measure of how such mutations affect repressor function.

Because Keap1 contains 25 cysteine residues, mutation of all possible combinations of cysteine residues was impractical, and we therefore mutated cysteines in selected domains. The BTB and DGR domains of Keap1 (see Fig. 1) are involved in dimerization (33) and Nrf-2/actin binding (19, 27), respectively; consequently, we did not mutate cysteine residues in these regions. The following groups of cysteine to alanine mutations were generated in Keap1: (*i*) N-terminal region (NTR), i.e., C23A and C38A, (*ii*) C-terminal region (CTR), i.e., C613A, C622A, and C624A, (*iii*) seven cysteines in the IVR, and (*iv*) 10 other combinations of mutations of these residues. Control cells were "mock" transfected with all constructs including the Keap1 expression vector, which lacked the cDNA sequence for Keap1.

In the absence of Keap1, the luciferase reporter of transfected cells showed high levels of luminescence (Fig. 4*a*). In agreement with previous studies (27), expression of increasing amounts of wild-type Keap1 in the presence of a constant amount of Nrf2 repressed the ARE-driven reporter luciferase activity in a concentration-dependent manner, and this repression was reversed by sulforaphane (Fig. 4*a*). Mutations of all cysteines in the N-terminal (NTR) or C-terminal (CTR) domains had no effect on the repressor activity of Keap1 (Fig. 4*b*). Thus, although C613 was labeled by Dex-mes, it is apparently not critical for the binding of Keap1 to Nrf2. In sharp contrast, mutants of Keap1 lacking either seven cysteine residues of the IVR (C226A–C297A), or four of these cysteines (C257A–C297A) cannot repress the expression of the luciferase reporter (Fig. 4*b*). This finding strongly suggests that the cysteine residues of Keap1 that are most reactive with an inducer are also those that influence binding and repression of Nrf2.

We next refined the mutation strategy to focus on the effects of mutating various combinations of the aforementioned seven cysteine residues of the IVR. Again mutation of both C226A–C257A and C297A did not disturb repressor activity, nor did mutation of C257A alone. The critical finding (Fig. 4*c*) is that absence of either C273 or C288 (or both) abrogates the repressor activity. Both of these cysteines react avidly with Dex-mes. C273 and C288 are flanked by basic amino acids (RC273H, and KC288E, respectively; see Fig. 1) which lower their pK_a values markedly, and thereby increase their reactivity (39). These results are pleasingly consistent with two very recent studies: Zhang and Hannink (21) showed that C273 or C288 are required for Keap1-dependent ubiquitination of Nrf2, and Levonen *et al.* (20) demonstrated that reactive thiols of Keap1 are targets of electrophilic lipid oxidation products, and mutation of C273 or C288 to serine renders Keap1 unable to prevent Nrf2 nuclear translocation.

The question of how mutation of either C273 or C288 could lead to loss of repressor function was further illuminated by experiments in which mixtures of vectors expressing each of these mutants were transfected simultaneously into the reporter system (Fig. 5). The striking finding was that, whereas each Keap1 mutant alone lacked repressor activity, transfection of a mixture of equal quantities of both of these Keap1 mutant expression vectors led to substantial restoration of repressor activity. This observation supports the view that Keap1 acts as a dimer and suggests that the simultaneous presence of C273 on one monomer and C288 on the other is compatible with repressor activity.

Formation of Intermolecular Disulfide Bonds by Binding of Phase 2 Enzyme Inducers to Keap1 in Cells. Our previous observation that reaction of Keap1 with stoichiometric equivalents of dipyridyl disulfide led to formation of two equivalents of pyridine thione (18) strongly suggested that the initially formed mixed disulfide between reagent and protein was rapidly reduced by another highly reactive cysteine thiol of Keap1 to form a disulfide linkage. To determine the oligomerization state of Keap1 after inducer treatment, we first transfected human embryonic kidney (HEK) 293 cells with the Keap1 vector and then exposed the cells to inducers for 6 h in serum-free medium. Inducers of three different types were used, i.e., the Michael reaction acceptor bis(2-hydroxybenzylidene)acetone, the isothiocyanate sulfora-

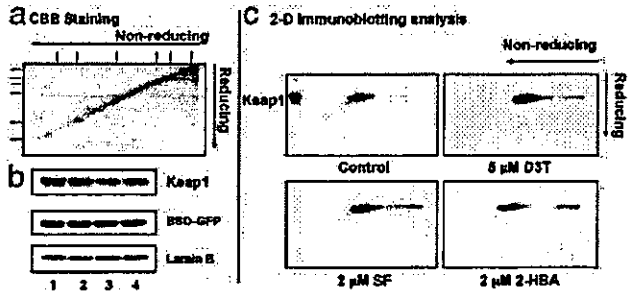

Fig. 6. Exposure to inducers causes formation of a disulfide-linked dimer of Keap1 in HEK 293 cells transfected with a construct encoding for Keap1 and GFP (normalization control). (*a*) Coomassie brilliant blue (CBB) staining of 2D SDS/PAGE of cell-free extracts. (*b*) Immunoblots of SDS/PAGE of control (lanes 1 and 2) and inducer-treated (lanes 3 and 4) cells showing (*Top*) reduced binding of the anti-Keap1 antibody for Keap1 in inducer-treated cells compared with control cells, (*Middle*) equal expression of GFP, and (*Bottom*) equal cell numbers as judged by the expression of Lamin B. (*c*) Immunoblots for Keap1 of 2D SDS/PAGE of extracts of control cells and cells exposed to inducers of three different chemical types. SF, sulforaphane; D3T, 1,2-dithiole-3-thione; 2-HBA, bis(2-hydroxybenzylidene)acetone.

phane, and 1,2-dithiole-3-thione. At the end of the exposure period, cell-free extracts were subjected to 2D SDS/PAGE (40) under nonreducing conditions in the first dimension and under reducing conditions (2-mercaptoethanol) in the second dimension. Western blot analysis was then used to localize Keap1 (Fig. 6). Only a single immunoreactive product corresponding to monomeric Keap1 was detected in uninduced cells. In contrast, the anti-Keap1 antibody recognized two products in extracts of cells treated with inducers, corresponding to a monomer and an intermolecular disulfide-linked dimer of Keap1 (Fig. 6*c*). This observation provides strong, independent evidence that reaction with inducers leads to the formation of intermolecular dimers between Keap1 subunits.

Comparison of the Keap1/Nrf2 System with Other Genes Regulated by Oxidative Stress and Sensed by Cysteine Thiol Groups. Although the behavior of the Keap1-Nrf2 system is in many ways unique, it resembles regulation of other proteins in which cysteine residues are modified. The prokaryotic transcription factors OxyR and SoxR are activated by oxidation, resulting in formation of intramolecular disulfide bonds in response to hydrogen peroxide and superoxide, respectively (41–44). In response to oxidants, two intramolecular disulfide bonds are formed and Zn is released from the redox-sensitive chaperone Hsp33, leading to large conformational changes which increase its affinity for protein folding intermediates, thus protecting them from oxidative damage (45, 46). Regulation of protein function can also occur by disulfide bond reduction as exemplified by activation of integrins that control cell adhesion and migration (47).

To our knowledge, the Keap1-Nrf2 system may be unique in that it depends on chemical modification of specific cysteine thiols and that the modifying agents then appear to be displaced by intermolecular sulfhydryl disulfide interchange to lead to a covalent disulfide dimer of Keap1. This eukaryotic system resembles the RsrA-SigR system from *Streptomyces coelicolor* (48–50). Both Keap1-Nrf2 and RsrA-SigR are essential components of signal transduction pathways involved in protection against oxidative stress and electrophiles by up-regulating systems that detoxify damaging agents, the Phase 2 gene products in mammals and the thioredoxin operon in *S. coelicolor*. Under basal conditions, both Keap1 and RsrA are negative regulators of the transcription factors Nrf2 and SigR, respectively. Oxidative stress or exposure to inducers disrupts the complexes,

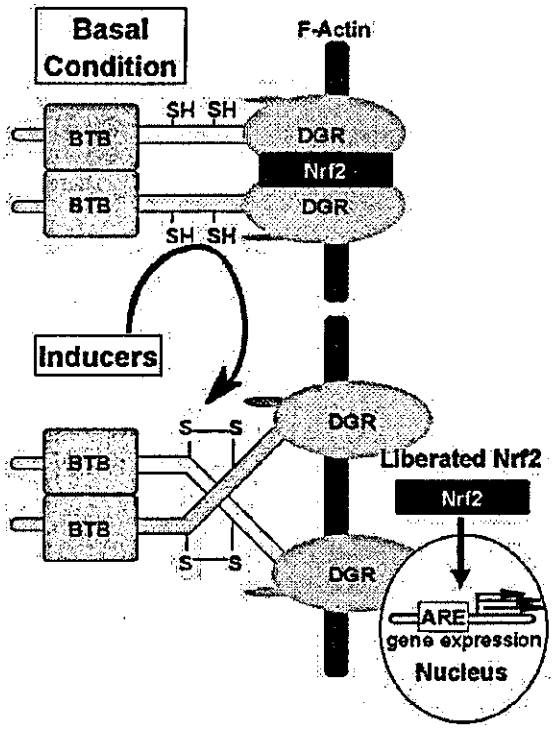

Fig. 7. Mechanism of regulation of the phase 2 response. Nrf2 (black) is retained in the cytoplasm by interaction with two molecules of Keap1, which are dimerized through their BTB domains (pink) and anchored to the actin cytoskeleton via the Kelch or DGR region (gray propeller). Inducers of the phase 2 response interact with cysteine thiol groups in the intervening region (IVR, yellow) of Keap1, causing the formation of disulfide bonds (most likely between C273 of one monomer and C288 of the other). This results in conformational change that renders Keap1 unable to bind to Nrf2, which then translocates to the nucleus. The Nrf2 in heterodimeric combination with other transcription factors such as small Maf binds to the ARE regulatory region of phase 2 genes and enhances their transcription.

allowing the transcription factors to activate gene expression via their respective enhancer elements. Deletion of the genes encoding for Keap1 or RsrA leads to constitutive activation of the transcription factors and overexpression of the genes that are under their control, even in the absence of any stimulus. Interestingly, the IVR of Keap1 is similar in size and cysteine content to the RsrA. Individual mutations of critical cysteines of Keap1 and RsrA render them unable to repress their partner transcription factors. In both cases, this finding was completely unexpected, because the wild-type repressors are active in the reduced state and the inability to form disulfide bond(s) by mutating the participating cysteine residues is expected to lock the repressor in its constitutively active form.

These two systems present a similar paradox: (*i*) the repressors are sensors of the signal and are therefore indispensable components in the signal transduction pathway leading to induction, but if they are absent (i.e., knocked out), the same inducible genes, instead of being uninducible, are constitutively up-regulated; (*ii*) specific cysteines must be able to form disulfide bonds for repressor activity, but disulfide formation leads to release of repression, pointing out that these cysteines are not only important for inducer sensing, but also for direct interaction between the two partner (repressor/transcription factor) molecules. Their modification, for example, by disulfide bond formation, can lead to conformational changes that do not allow binding to occur. In RsrA, the critical cysteines are involved in

Zn coordination that controls the thiol-disulfide reactivity of RsrA, the Zn is expelled during oxidation with concomitant disulfide bond formation that then causes major conformational changes and does not allow binding to SigR. It is conceivable that C273 and C288 from each monomer are involved in metal coordination that, in addition to the proximity of these cysteines to basic amino acid residues, can stabilize the negative charges on the thiolate anions, lower their pK_a values, and explain their unusually high reactivity.

Summary. These results are consistent with the model shown in Fig. 7. Under basal (reducing) conditions, Keap1 exists as a dimer in which two monomers are bound to each other, possibly by hydrophobic interactions via their BTB domains. The cysteines C273 and C288 of the intervening region are in the reduced state. In this conformation Keap1 sequesters one molecule of Nrf2 between two DGR domains in the cytoplasm and ensures its rapid turnover by targeting to the proteasome. Upon exposure to inducers, the reactive C273 and C288 residues form intermolecular disulfide bonds, thus covalently linking two monomers of Keap1. The resulting conformation separates the DGR domains, liberates Nrf2, and allows its translocation to the nucleus and enhanced expression of phase 2 genes.

We thank Philip A. Cole, Jed W. Fahey, and James T. Stivers for much perceptive advice. Robert N. Cole provided consultation and advice on the matrix-assisted laser desorption ionization/time-of-flight mass spectrometry, Osamu Ohneda helped in establishing the cell lines from the knockout mice, and Pamela Talalay provided valuable editorial consultation. These studies were supported by grants from the National Cancer Institute, Department of Health and Human Services (Grant CA 94076), the American Institute for Cancer Research (Washington, DC), and the Brassica Foundation for Cancer Chemoprotection Research (Baltimore). The AB-Mass Spectrometry Facility at the Johns Hopkins School of Medicine is funded by National Center for Research Resources Shared-Instrumentation Grant 1S10-RR14702. These studies were also supported by generous gifts from the Lewis B. and Dorothy Cullman Foundation, the Barbara Lubin Goldsmith Foundation, and the McMullan Family Fund.

1. Hayes, J. D. & McLellan, L. I. (1999) *Free Radical Res.* **31**, 273–300.
2. Talalay, P., Dinkova-Kostova, A. T. & Holtzclaw, W. D. (2003) *Adv. Enzyme Regul.* **43**, 121–134.
3. Talalay, P. (1999) *Proc. Am. Philos. Soc.* **143**, 52–72.
4. Talalay, P. (2000) *Biofactors* **12**, 5–11.
5. Ramos-Gomez, M., Kwak, M. K., Dolan, P. M., Itoh, K., Yamamoto, M., Talalay, P. & Kensler, T. W. (2001) *Proc. Natl. Acad. Sci. USA* **98**, 3410–3415.
6. Fahey, J. W., Haristoy, X., Dolan, P. M., Kensler, T. W., Scholtus, I., Stephenson, K. K., Talalay, P. & Lozniewski, A. (2002) *Proc. Natl. Acad. Sci. USA* **99**, 7610–7615.
7. Cho, H. Y., Jedlicka, A. E., Reddy, S. P., Kensler, T. W., Yamamoto, M., Zhang, L. Y. & Kleeberger, S. R. (2002) *Am. J. Respir. Cell Mol. Biol.* **26**, 175–182.
8. Henderson, C. J., Smith, A. G., Ure, J., Brown, K., Bacon, E. J. & Wolf, C. R. (1998) *Proc. Natl. Acad. Sci. USA* **95**, 5275–5280.
9. Long, D. J., Jr., Waikel, R. L., Wang, X. J., Perlaky, L., Roop, D. R. & Jaiswal, A. K. (2000) *Cancer Res.* **60**, 5913–5915.
10. Clairmont, A., Sies, H., Ramachandran, S., Lear, J. T., Smith, A. G., Bowers, B., Jones, P. W., Fryer, A. A. & Strange, R. C. (1999) *Carcinogenesis* **20**, 1235–1240.
11. Lafuente, M. J., Casterad, X., Trias, M., Ascaso, C., Molina, R., Ballesta, A., Zheng, S., Wiencke, J. K. & Lafuente, A. (2000) *Carcinogenesis* **21**, 1813–1819.
12. Smith, M. T., Wang, Y., Skibola, C. F., Slater, D. J., Lo Nigro, L., Nowell, P. C., Lange, B. J. & Felix, C. A. (2002) *Blood* **100**, 4590–4593.
13. Zhang, J., Schulz, W. A., Li, Y., Wang, R., Zotz, R., Wen, D., Siegel, D., Ross, D., Gabbert, H. E. & Sarbia, M. (2003) *Carcinogenesis* **24**, 905–909.
14. Kensler, T. W., Qian, G.-S., Chen, J.-G. & Groopman, J. D. (2003) *Nat. Rev. Cancer* **3**, 321–329.
15. Talalay, P., De Long, M. J. & Prochaska, H. J. (1988) *Proc. Natl. Acad. Sci. USA* **85**, 8261–8265.
16. Prestera, T., Zhang, Y., Spencer, S. R., Wilczak, C. A. & Talalay, P. (1993) *Adv. Enzyme Regul.* **33**, 281–296.
17. Dinkova-Kostova, A. T., Massiah, M. A., Bozak, R. E., Hicks, R. J. & Talalay, P. (2001) *Proc. Natl. Acad. Sci. USA* **98**, 3404–3409.
18. Dinkova-Kostova, A. T., Holtzclaw, W. D., Cole, R. N., Itoh, K., Wakabayashi, N., Katoh, Y., Yamamoto, M. & Talalay, P. (2002) *Proc. Natl. Acad. Sci. USA* **99**, 11908–11913.
19. Kang, M.-I., Kobayashi, A., Wakabayashi, N., Kim, S.-G. & Yamamoto, M. (2004) *Proc. Natl. Acad. Sci. USA* **101**, 2046–2051.
20. Levonen, A.-L., Landar, A., Ramachandran, A., Ceaser, E. K., Dickinson, D. A., Zanoni, G., Morrow, J. D. & Darley-Usmar, V. M. (2003) *Biochem. J.*, in press.
21. Zhang, D. D. & Hannik, M. (2003) *Mol. Cell. Biol.* **23**, 8137–8151.
22. Hayes, J. D. & McMahon, M. (2001) *Cancer Lett.* **174**, 103–113.
23. Nguyen, T., Sherratt, P. J. & Pickett, C. B. (2003) *Annu. Rev. Pharmocol. Toxicol.* **43**, 233–260.
24. Chui, D. H., Tang, W. & Orkin, S. H. (1995) *Biochem. Biophys. Res. Commun.* **209**, 40–46.
25. Itoh, K., Chiba, T., Takahashi, S., Ishii, T., Igarashi, K., Katoh, Y., Oyake, T., Hayashi, N., Satoh, K., Hatayama, I., *et al.* (1997) *Biochem. Biophys. Res. Commun.* **236**, 313–322.
26. Venugopal, R. & Jaiswal, A. K. (1996) *Proc. Natl. Acad. Sci. USA* **93**, 14960–14965.
27. Itoh, K., Wakabayashi, N., Katoh, Y., Ishii, T., Igarashi, K., Engel, J. D. & Yamamoto, M. (1999) *Genes Dev.* **13**, 76–86.
28. Itoh, K., Wakabayashi, N., Katoh, Y., Ishii, T., O'Connor, T. & Yamamoto, M. (2003) *Genes Cells.* **8**, 379–391.
29. McMahon, M., Itoh, K., Yamamoto, M. & Hayes, J. D. (2003) *J. Biol. Chem.* **278**, 21592–21600.
30. Nguyen, T., Sherratt, P. J., Huang, H. C., Yang, C. S. & Pickett, C. B. (2003) *J. Biol. Chem.* **278**, 4536–4541.
31. Sekhar, K. R., Yan, X. X. & Freeman, M. L. (2002) *Oncogene* **21**, 6829–6834.
32. Stewart, D., Killeen, E., Naquin, R., Alam, S. & Alam, J. (2003) *J. Biol. Chem.* **278**, 2396–2402.
33. Zipper, L. M. & Mulcahy, R. T. (2002) *J. Biol. Chem.* **277**, 36544–36552.
34. Prag, S. & Adams, J. C. (2003) *BMC Bioinformatics* **4**, 42.
35. Hogan, B., Constantini, F. & Lacy, Y. (1986) *Manupulating the Mouse Embryo: A Laboratory Manual* (Cold Spring Harbor Lab. Press, Plainview, NY).
36. Wakabayashi, N., Itoh, K., Wakabayashi, J., Motohashi, H., Noda, S., Takahashi, S., Imakado, S., Kotsuji, T., Otsuka, F., Roop, D. R., *et al.* (2003) *Nat. Genet.* **35**, 238–245.
37. Zhang, Y. & Callaway, E. C. (2002) *Biochem J.* **364**, 301–307.
38. Favreau, L. V.& Pickett, C. B. (1995) *J. Biol. Chem.* **270**, 24468–24474.
39. Snyder, G. H., Cennerazzo, M. J., Karalis, A. J. & Field, D. (1981) *Biochemistry* **20**, 6509–6519.
40. Hynes, R. O. & Destree, A. (1977) *Proc. Natl. Acad. Sci. USA* **74**, 2855–2859.
41. Zheng, M., Aslund, F. & Storz, G. (1988) *Science* **279**, 1718–1721.
42. Zheng, M. & Storz, G. (2000) *Biochem. Pharmacol.* **59**, 1–6.
43. Sun, Y. & Oberley, L. W. (1996) *Free Radical Biol. Med.* **21**, 335–348.
44. Georgiou, G. (2002) *Cell* **111**, 607–610.
45. Graumann, J., Lilie, H., Tang, X., Tucker, K. A., Hoffmann, J. H., Vijayalakshmi, J., Saper, M., Bardwell, J. C. & Jakob, U. (2001) *Structure (Cambridge, Mass.)* **9**, 377–387.
46. Linke, K. & Jakob, U. (2003) *Antioxid. Redox Signal.* **5**, 425–434.
47. Yan, B. & Smith, S. W. (2001) *Biochemistry* **40**, 8861–8867.
48. Kang, J.-G., Paget, M. S. B., Seok, Y.-J., Hahn, M.-Y., Bae, J.-B., Hahn, J.-S., Kleanthous, C., Buttner, M. J. & Roe, J.-H. (1999) *EMBO J.* **18**, 4292–4298.
49. Paget, M. S., Bae, J. B., Hahn, M. Y., Li, W., Kleanthous, C., Roe, J. H. & Buttner, M. J. (2001) *Mol. Microbiol.* **39**, 1036–1047.
50. Li, W., Bottrill, A. R., Bibb, M. J., Buttner, M. J., Paget, M. S. & Kleanthous, C. (2003) *J. Mol. Biol.* **333**, 461–472.

Scaffolding of Keap1 to the actin cytoskeleton controls the function of Nrf2 as key regulator of cytoprotective phase 2 genes

Moon-Il Kang*†, Akira Kobayashi*†, Nobunao Wakabayashi*, Sang-Geon Kim‡, and Masayuki Yamamoto*†§

*Center for Tsukuba Advanced Research Alliance and †Japan Science and Technology Agency–Exploratory Research for Advanced Technology Environmental Response Project, University of Tsukuba, 1-1-1 Tennoudai, Tsukuba 305-8575, Japan; and ‡National Research Laboratory, College of Pharmacy and Research Institute of Pharmaceutical Sciences, Seoul National University, Seoul 151-742, Korea

Communicated by Paul Talalay, Johns Hopkins University School of Medicine, Baltimore, MD, December 16, 2003 (received for review November 8, 2003)

Transcription factor Nrf2 regulates basal and inducible expression of phase 2 proteins that protect animal cells against the toxic effects of electrophiles and oxidants. Under basal conditions, Nrf2 is sequestered in the cytoplasm by Keap1, a multidomain, cysteine-rich protein that is bound to the actin cytoskeleton. Keap1 acts both as a repressor of the Nrf2 transactivation and as a sensor of phase 2 inducers. Electrophiles and oxidants disrupt the Keap1–Nrf2 complex, resulting in nuclear accumulation of Nrf2, where it enhances the transcription of phase 2 genes via a common upstream regulatory element, the antioxidant response element. Reporter cotransfection–transactivation analyses with a series of Keap1 deletion mutants revealed that in the absence of the double glycine repeat domain Keap1 does not bind to Nrf2. In addition, deletion of either the intervening region or the C-terminal region also abolished the ability of Keap1 to sequester Nrf2, indicating that all of these domains contribute to the repressor activity of Keap1. Immunocytochemical and immunoprecipitation analyses demonstrated that Keap1 associates with actin filaments in the cytoplasm through its double glycine repeat domain. Importantly, disruption of the actin cytoskeleton promotes nuclear entry of an Nrf2 reporter protein. The actin cytoskeleton therefore provides scaffolding that is essential for the function of Keap1, which is the sensor for oxidative and electrophilic stress.

Oxidative and electrophilic stresses provoke physiological responses that induce the expression of various cytoprotective genes (1). Recently, the transcription factor Nrf2 (2) or ECH (3) was identified as the major regulator of the cytoprotective genes encoding phase 2 detoxication and antioxidant enzymes (4, 5). Nrf2, a basic region–leucine zipper (b-Zip) transcription factor (6) contains the N-terminal Neh2 domain, which is conserved between human Nrf2 (2) and chicken ECH (3). Biochemical analyses further revealed that the Neh2 domain serves as a negative regulatory domain of Nrf2 transcriptional activity, and we subsequently isolated a protein, Keap1, as an Neh2-associated protein (7).

Keap1 shares close similarity with *Drosophila* Kelch protein, which is essential for the formation of actin-rich intracellular bridges termed ring canals (8). These proteins have two common characteristic domains, i.e., the BTB (Broad complex, Tramtrack, and Bric a Brac)/POZ (poxvirus and zinc finger) and double glycine repeat (DGR or Kelch repeats) domains at the N- and C-terminal regions (NTR and CTR), respectively. The BTB domain of Keap1 has been examined in a transfection assay and was shown to be important for Keap1 function (9). The DGR domain comprises six repeats of the Kelch motif, and according to the x-ray structural analysis of galactose oxidase, which is a protein containing a Kelch motif, Kelch repeats form β-propeller structures (10). Importantly, many Kelch-related proteins colocalize with actin filaments through the Kelch repeats, suggesting a biological role of the DGR domain in the regulation and maintenance of the cytoskeleton (11, 12).

The association of Nrf2 with Keap1 has been examined (7). In the absence of electrophiles or oxidants, Nrf2 localizes in the cytoplasm in association with Keap1. On exposure to these inducers, however, Keap1 liberates Nrf2, allowing it to translocate to the nucleus and transactivate cytoprotective genes. Germline Nrf2-deficient mice have significantly reduced inducible and/or basal level expression of phase 2 and antioxidant enzymes compared with wild-type mice (4, 5). Deficient expression of cytoprotective enzymes renders mice highly sensitive to carcinogens and oxidative stresses, demonstrating that Nrf2 plays major roles in the defense systems against chemical carcinogenesis and acute drug intoxication (reviewed in refs. 1 and 13).

We also generated germline Keap1-deficient mice (14). Although homozygous *Keap1* mutant newborns appeared normal, they all died within 3 weeks after birth. Detailed postmortem analyses revealed severe hyperkeratosis in the esophagus and forestomach of these mutants. We found that the Keap1–Nrf2 pathway also regulates a subset of genes induced in squamous cell epithelia in response to mechanical stress. Importantly, all of the Keap1-dependent phenotypes were reversed in *Keap1–Nrf2* combined null-mutant mice, indicating that the Keap1 deficiency caused Nrf2 to accumulate constitutively accumulate in the nucleus. These results thus establish that the Keap1–Nrf2 system is an essential regulatory pathway that controls the cellular response to oxidative and xenobiotic stresses.

These *in vivo* examinations led us to address the next important question: how signals from oxidants and electrophiles are transmitted to the Keap1–Nrf2 system. Because the only common chemical property of phase 2 inducers is their ability to react with sulfhydryl groups, it has been proposed that the inducers may react with cysteine residues of a sensor protein (15). Indeed, Keap1 contains 25 cysteine residues, some of which have the characteristics of reactive cysteine. Phase 2 inducers react with sulfhydryl groups of Keap1, resulting in the disruption of the Keap1–Nrf2 complex (23). Hence, we envisage that Keap1 may function as one of the stress sensors in eukaryotes. Here, we describe the molecular mechanisms whereby Keap1 regulates Nrf2 activity under unstressed conditions. We identified five domains of Keap1 that may have discrete functions. These domains are referred to as N-terminal region (NTR), BTB, intervening region (IVR), DGR, and C-terminal region (CTR). In closer structure–function analyses of these domains, we found that Keap1 interacts with the actin filaments through DGR and that this interaction is crucial for Keap1 activity. We also found

Abbreviations: ARE, antioxidant response element; BTB, Broad complex, Tramtrack, and Bric-a-Brac; CTR, C-terminal region; DGR, double glycine repeat; IVR, intervening region; NTR, N-terminal region.

§To whom correspondence should be addressed at: Center for Tsukuba Advanced Research Alliance, University of Tsukuba, 1-1-1 Tennoudai, Tsukuba 305-8575, Japan. E-mail: masi@tara.tsukuba.ac.jp.

www.pnas.org/cgi/doi/10.1073/pnas.0308347100

that both IVR and CTR are essential for Keap1 to retain Nrf2 in the cytoplasm. Taken together, these data demonstrate that the Keap1–Nrf2 system provides a unique biological regulatory mechanism, formed through interaction with the actin filament network.

Experimental Procedures

Plasmid Construction. Full-length mouse Keap1 cDNA was subcloned into pcDNA3 (Invitrogen) vector (pcDNA-mKeap1). Keap1 deletion mutants were generated by inserting appropriate PCR-amplified cDNA fragments into the pcDNA3 vector. Information on the primers is available on request. These mutants were named ΔNTR (amino acids 1–60 deleted), ΔBTB (amino acids 61–179 deleted), ΔIVR (amino acids 192–308 deleted), ΔDGR (amino acids 315–598 deleted), and ΔCTR (amino acids 599–624 deleted). Structures of all constructs were verified by DNA sequencing.

Transfection Experiments and Luciferase Assay. Transfection experiments were performed as described (7) by using Lipofectamine plus reagents (Invitrogen). Luciferase assay was performed by using the Dual-Luciferase reporter assay system (Promega). Expression plasmids of Keap1 deletion mutants and Nrf2 were transfected into NIH 3T3 cells along with pNQO1 (nicotinamide quinone oxidoreductase 1)-ARE (antioxidant response element) reporter plasmid and pRL-TK as a control. pNQO1-ARE plasmid contains a single ARE and was used to measure the transactivation activity of Nrf2.

Laser Confocal Scanning Microscopy. A mouse Keap1 cDNA fragment was inserted into pCAGGS vector (pCAGGS-mKeap1; ref. 17). The resultant plasmid was injected into fertilized eggs and mouse embryonic fibroblasts (MEF) were prepared from transgene-positive 14.5-day-old embryos. Subcellular localization of Keap1 and actin was examined by immunohistochemical staining with laser confocal microscope (Leica). Anti-Keap1 antibodies were raised in rabbits by a standard method by using oligopeptides against the N and C termini of Keap1 individually.

Immunohistochemical Staining. Expression plasmids of Neh2-GFP and Keap1 deletion mutants were transfected into NIH 3T3 cells grown on slides. Cells were washed and fixed 36 h after transfection as described (7). Actin filament disruption experiments were modified from previous methods (18–21). In brief, cells were incubated with cytochalasin B (6 μM), swinholide A (50 nM), or colchicines (1 μM) for several periods of time as described in the figure legends. Cells were washed with PBS, blocked with 2% goat serum, and treated with anti-Keap1 antibody (100-fold dilution). Cells were then treated with goat anti-rabbit IgG conjugated with tetramethylrhodamine B isothiocyanate (TRITC, Zymed), 4′,6-diamidino-2-phenylindole (DAPI, 200 ng/ml), and Texas red-X phalloidin (200 units/ml, Molecular Probes). After washing with PBS, a drop of fluorescent mounting medium (DAKO) was placed on the slides.

Immunoprecipitation Analysis. 293T cells expressing Keap1 deletion mutants and Flag-Nrf2 were grown on culture dishes. Cells were harvested with Harlow buffer (50 mM Tris·HCl, pH 7.5/1% Nonidet P-40/20 mM EDTA/50 mM NaF) supplemented with protease inhibitors (Roche Diagnostics). Cell extracts were first cleared with protein G Sepharose and incubated with ANTI-FLAG M2 affinity gel (Sigma) or anti-actin (C-2) mouse monoclonal IgG (Santa Cruz Biotechnology) bound to protein G Sepharose. The immunocomplexes were washed five times with Harlow solution and subjected to immunoblot analysis.

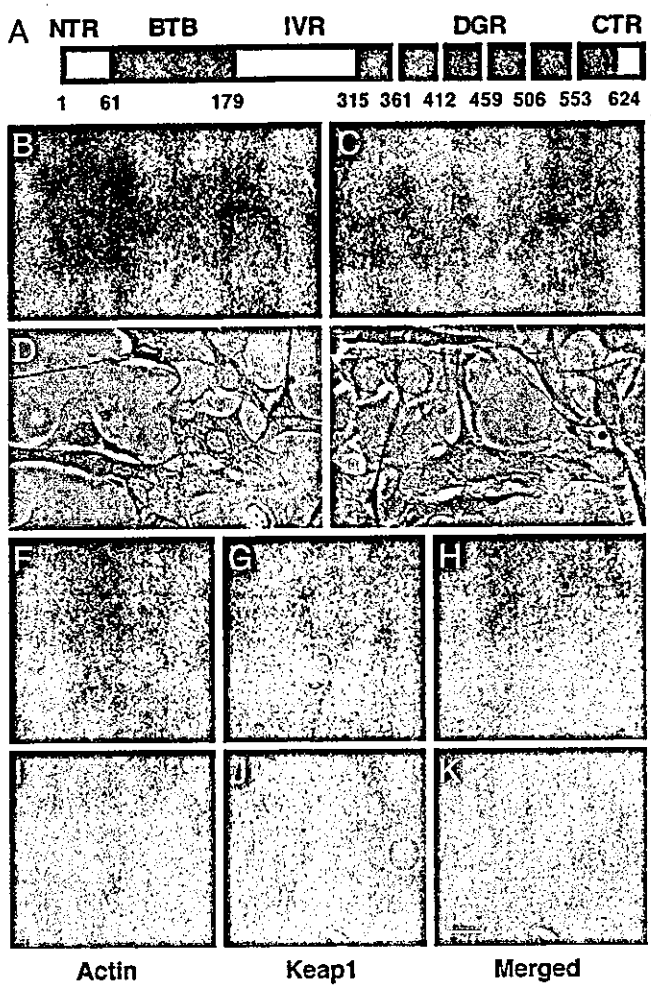

Fig. 1. Keap1 colocalizes with actin filaments in the cytoplasm. (*A*) Schematic presentation of Keap1 based on Swiss-Prot, using the Sanger Center Database. We assigned five domains within Keap1: NTR, BTB, IVR, DGR, and CTR. (*B–E*) Cytoplasmic localization of Keap1 in NIH 3T3 cells. Keap1 was expressed in NIH 3T3 cells, and subcellular localization of Keap1 was detected immunohistochemically by two anti-Keap1 antibodies against the N- and C-terminal ends of Keap1 (*B* and *C*, respectively). Bright-field microscopic images for *B* and *C* are shown in *D* and *E*, respectively. (*F–K*) colocalization of Keap1 and actin filaments in MEF derived from transgenic mouse embryos expressing Keap1. Subcellular localization of actin filaments (*F* and *I*) and Keap1 (*G* and *J*) are visualized by staining with phalloidin conjugated with Texas red and anti-Keap1 antibody, respectively. *H* and *K* show merged signals. Fluorescence was recorded by confocal microscopy. (Scale bar, 40 μm.)

Results

Keap1 Functions as an Actin-Binding Protein. To clarify the molecular mechanisms of Keap1 function, we first investigated the functional domains of Keap1. Comparison of the amino acid sequences of mouse, rat, and human (KIAA0132) Keap1 proteins shows that their sequences are highly conserved (>94%) among these species (data not shown). Pfam database (q9z2x8, mouse Keap1) analyses indicate that Keap1 protein consists of five characteristic domains: NTR, BTB/POZ, IVR, DGR, and CTR (Fig. 1*A*). The DGR structure also exists in other Kelch-related proteins, and some of them, such as Mayven (22), have been reported to interact with actin filaments through DGR. These data led us to examine whether Keap1 might act as an actin-binding protein.

We examined the colocalization of Keap1 with actin filaments in the cytoplasm. We raised two anti-Keap1 antibodies, which

recognize either the N-terminal or the C-terminal end regions of Keap1. Keap1 expression plasmid was transfected into NIH 3T3 cells, and the subcellular localization of Keap1 was monitored by immunocytochemical staining with anti-Keap1 antibodies. Both anti-N terminus antibody (Fig. 1 *B* and *D*) and anti-C terminus antibody (*C* and *E*) recognized Keap1 as a cytoplasmic factor. The localization of the signals suggests a fiber-based distribution of Keap1.

The subcellular localization of Keap1 was examined by confocal microscopy. Because the expression level of endogenous Keap1 was below the detection limit of the antibodies, for this analysis we prepared transgenic mice that express Keap1 at relatively high levels under the regulation of the CAGGS promoter (17). We assumed that overexpression of Keap1 in transgenic mouse embryos would reflect the physiological localization of Keap1 more closely than overexpression in cultured cells. Overexpression of Keap1 in transgenic mice did not affect the development or growth of the mice (data not shown). Immunostaining of mouse embryonic fibroblasts (MEF) derived from the transgenic embryos with the mixture of anti-Keap1 antibodies is shown in Fig. 1 (*F–K*) along with the staining of actin filaments with phalloidin conjugated with Texas red. Keap1 was localized in the perinuclear region and showed a fibrous pattern (*G* and *J*); and expression of Keap1 appeared to overlap that of the actin filaments (*F* and *I*). When we merged the two staining patterns, they overlapped markedly (*H* and *K*). The overlapping image (yellow) is more pronounced in the perinuclear region than in the region beneath the plasma membrane. Thus, these data suggest that Keap1 may bind directly to the actin filaments or cytoskeleton in the cytoplasm.

Direct Association of Keap1 with Actin Through DGR. To address whether Keap1 and actin filaments interact directly, we performed an immunoprecipitation analysis by using whole-cell extracts of 293T cells expressing a series of Keap1 deletion mutants (Fig. 2*A*). Precipitates obtained by anti-actin antibody were subjected to immunoblot analysis with anti-Keap1 antibodies. As shown in Fig. 2*B*, Keap1 was detected in the complex precipitated by the anti-actin antibody (*Upper*, lane 1), indicating that Keap1 and actin filaments interact directly.

To identify the surface of Keap1 interacting with actin, we carried out similar analyses with a series of Keap1 deletion mutants. The anti-actin antibody precipitated ΔNTR, ΔBTB, ΔIVR, and ΔCTR mutant proteins (Fig. 2*B*, lanes 2–5) but not the ΔDGR mutant protein (lane 7). Immunoblotting analysis with the anti-Keap1 antibodies indicated the presence of ΔDGR Keap1 protein as well as other mutant proteins in the whole-cell extracts (Fig. 2*B Lower*). These results demonstrate that DGR is the domain primarily responsible for the interaction of Keap1 with actin filaments.

Keap1 Requires Actin Filaments as Scaffolding. The results described above indicate that Keap1 retains Nrf2 in the cytoplasm under unstressed conditions. To elucidate whether the Keap1 activity requires actin filaments as scaffolding, we disrupted the actin cytoskeleton and examined the effect on the subcellular localization of Nrf2. NIH 3T3 cells were treated with cytochalasin B or swinholide A, which inhibit polymerization of actin filaments, and stained with phalloidin. Because prolonged treatment of NIH 3T3 cells (>12 h) with these compounds induced cell death (data not shown), we treated the cells with these reagents for <3 h and analyzed the effects. As a negative control, we also used colchicine, a specific inhibitor of microtubule polymerization. As shown in Fig. 3, treatment of NIH 3T3 cells with cytochalasin B or swinholide A disrupted the actin filament network effectively within 3 h (Fig. 3 *A–C*), whereas that with colchicine did not (Fig. 3*D*).

We then examined the effect of actin disruption on localization of Neh2-GFP containing GFP fused to the Neh2 domain in NIH 3T3 cells. Because we previously established that the Neh2 domain is the interactive interface of Nrf2 with Keap1 (7), we used this fusion protein as a reporter for the expression site of Nrf2. The subcellular localization of Neh2-GFP and Keap1 were monitored by the green fluorescence of GFP and immunostaining with anti-Keap1 antibodies, respectively. Whereas Neh2-GFP was localized exclusively in the cytoplasm in the presence of Keap1 (Fig. 3 *E* and *F*, 0 h), treatment with cytochalasin B resulted in an ≈5-fold increase in nuclear translocation of Neh2-GFP within 1 h. Additional incubation of the cells for 2 and 3 h with these reagents did not further enhance the entry of Neh2-GFP into the nucleus. The results are summarized in Fig. 3*F*. Subcellular localization of Neh2-GFP and Keap1 after treatment with swinholide A showed essentially similar profiles (Fig. 3*F*). In contrast, treatment with colchicine did not affect significantly the subcellular localization of Neh2-GFP (Fig. 3*F*, black bars). These results establish that disruption of the actin filament network releases Neh2-GFP from Keap1, resulting in entry of Neh2-GFP into the nucleus, thereby supporting our contention that Keap1 requires the actin cytoskeleton as a scaffold to sequester Nrf2 efficiently in the cytoplasm.

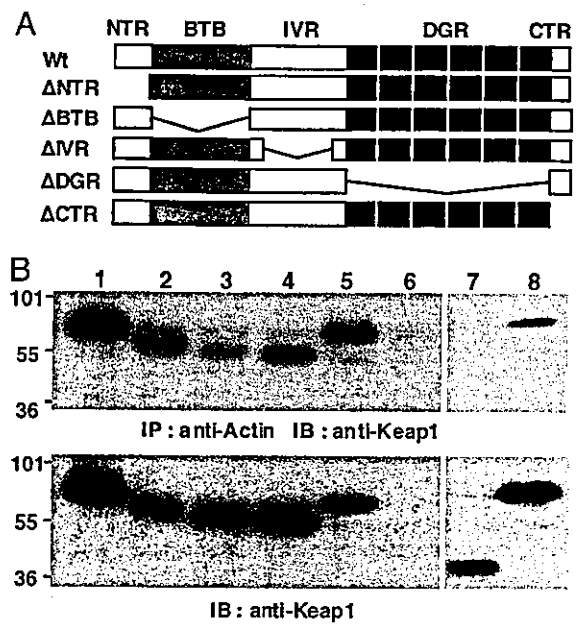

Fig. 2. Keap1 interacts with actin filaments through the DGR domain. (*A*) Schematic presentation of the structure of Keap1 deletion mutants. (*B*) Immunoprecipitation with whole-cell extracts of 293T cells expressing deletion mutants of Keap1. Immunoprecipitates (IP) obtained by anti-actin antibody were subjected to immunoblot analysis (IB) with anti-Keap1 antibody (*Upper*). The expression level of Keap1 deletion mutants was verified by immunoblot analysis (*Lower*). Analysis with wild-type Keap1-transfected cell lysates (lanes 1 and 8) as well as cell lysates transfected with Keap1 mutant ΔNTR (lane 2), ΔBTB (lane 3), ΔIVR (lane 4), ΔCTR (lane 5), and ΔDGR (lane 7) are shown. Lane 6 is loaded with cell extract expressing Nrf2 but not Keap1. Two anti-Keap1 antibodies were used: one against CTR (lanes 1–6) and the other against NTR (lanes 7 and 8).

Identification of a New Function of CTR. We examined the domain function of Keap1 further by expressing Keap1 deletion mutants (see Fig. 2*A*) and Neh2-GFP. Immunocytochemical staining with anti-Keap1 antibodies showed that all deletion mutants of Keap1 were localized in the cytoplasm (Fig. 4). In addition, wild-type Keap1 as well as ΔNTR, ΔBTB, and ΔIVR mutants localized Neh2-GFP exclusively in the cytoplasm, whereas ΔDGR and ΔCTR mutants of Keap1 did not. These results

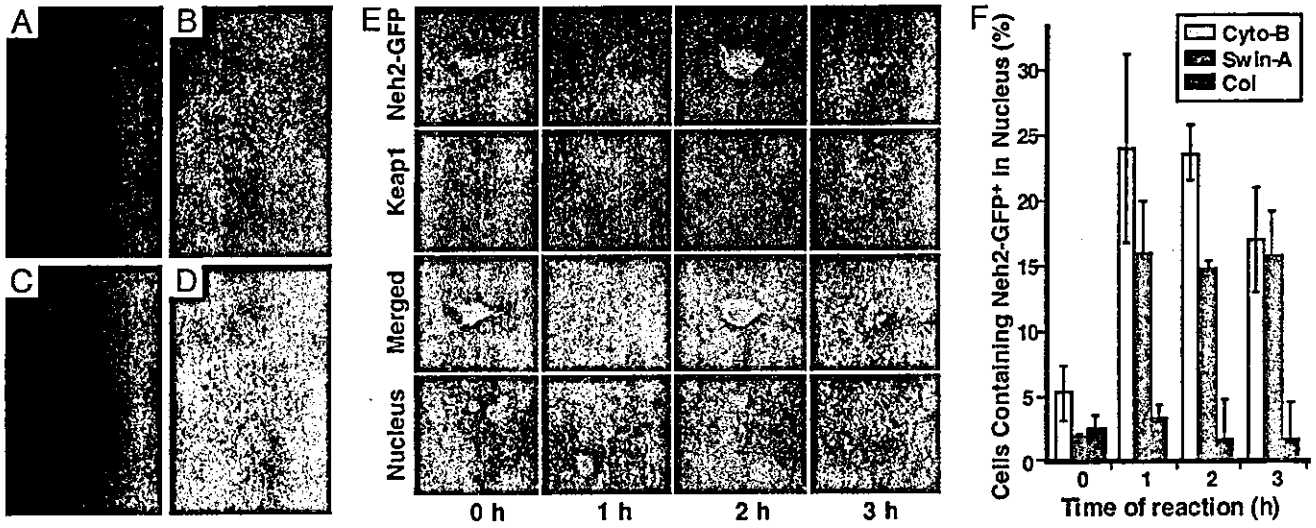

Fig. 3. Disruption of actin filaments triggers nuclear transport of Neh2-GFP. (*A*) NIH 3T3 cells were stained with phalloidin conjugated with Texas red and 4′,6-diamidino-2-phenylindole (DAPI) after addition of DMSO (*A*; a vehicle control) or cytoskeletal filament disruptors, cytochalasin B (*B*), swinholide A (*C*), or colchicine (*D*). (*E*) subcellular localization of Neh2-GFP and Keap1 after treatment with cytochalasin B. Cells (4×10^3) were transfected with expression plasmids of Keap1 (0.2 μg) and Neh2-GFP, a reporter protein of Nrf2 (0.8 μg). The latter is a fusion protein of Neh2 domain and GFP. Localization of these proteins was examined by fluorescence microscopy with use of GFP fluorescence and anti-Keap1 antibody, respectively (first and second rows). Merged images of Neh2-GFP and Keap1 signals are shown in the third row. Nuclei are shown with DAPI staining (fourth row). (Original magnification, ×400.) (*F*) nuclear transport of Neh2-GFP 3 h after the addition of cytochalasin B (Cyto-B), swinholide A (Swin-A), and colchicine (Col). Shown is the percentage of cells expressing Neh2-GFP in nucleus among the total transfected cells. The average and standard errors represent three independent transfection experiments.

suggest that in addition to DGR, CTR is also critical for Keap1 to retain Nrf2 in the cytoplasm.

DGR, but Not CTR, Directly Associates with Nrf2. We examined the direct interaction of each domain of Keap1 with Nrf2 by immunoprecipitation. Whole-cell extracts of 293T cells expressing a series of Keap1 deletion mutants and Flag-tagged Nrf2 were subjected to immunoprecipitation analysis by using anti-Flag antibody and then immunoblot analysis with anti-Keap1 antibodies. Consistent with the results in Fig. 4, deletion of DGR completely abolished the association of Keap1 with Nrf2 (Fig. 5*A*, lane 8). The amount of Nrf2 in the whole-cell extracts was monitored by immunoblot analysis with anti-Nrf2 antibody (Fig. 5*B*). Thus, DGR appears to be indispensable for interaction with both Nrf2 and actin filaments.

Surprisingly, the ΔCTR mutant interacted with Nrf2 in this immunoprecipitation analysis (Fig. 5*A*, lane 7), although this mutant did not retain Neh2-GFP in the cytoplasm (Fig. 4, ΔCTR). One plausible explanation for this discrepancy is that the CTR domain may modulate the conformation of DGR *in vivo* and thus regulate the interaction between Keap1 and Nrf2.

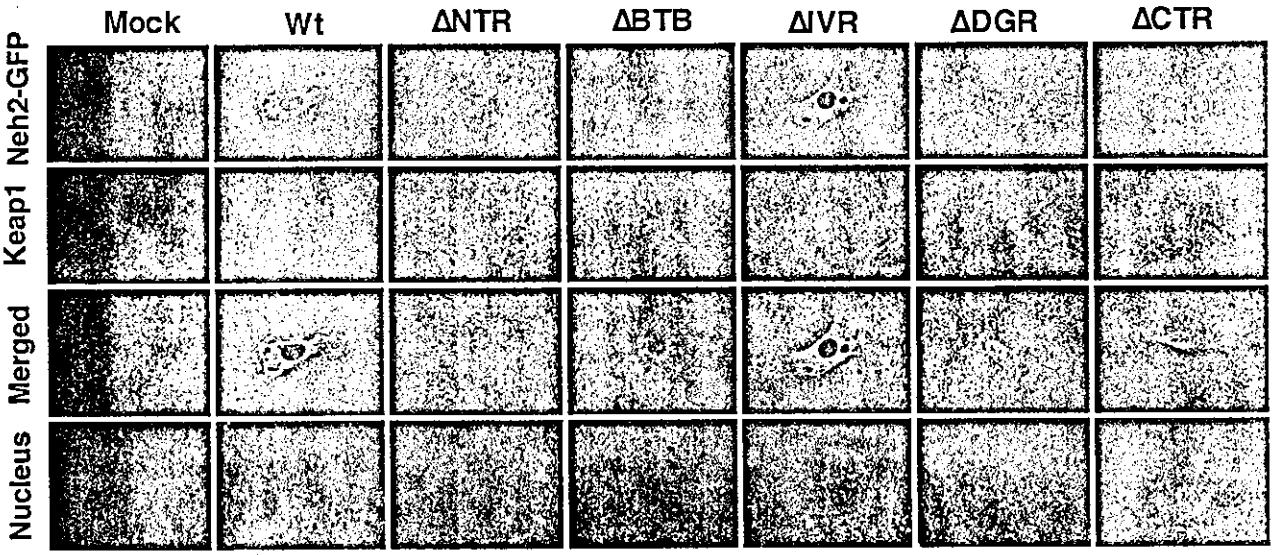

Fig. 4. CTR contributes to Keap1 activity retaining Neh2-GFP in cytoplasm. Subcellular localization of Neh2-GFP was examined in the presence of Keap1 deletion mutants. Transfection was performed as described in the legend to Fig. 3. Localization of Neh2-GFP and Keap1 mutant proteins was examined by fluorescence microscopy (first and second rows). Merged signals of both Neh2-GFP and Keap1 are shown in the third row. Nuclei are shown with DAPI staining (shown as Nucleus; fourth row). (Original magnification, ×400.)

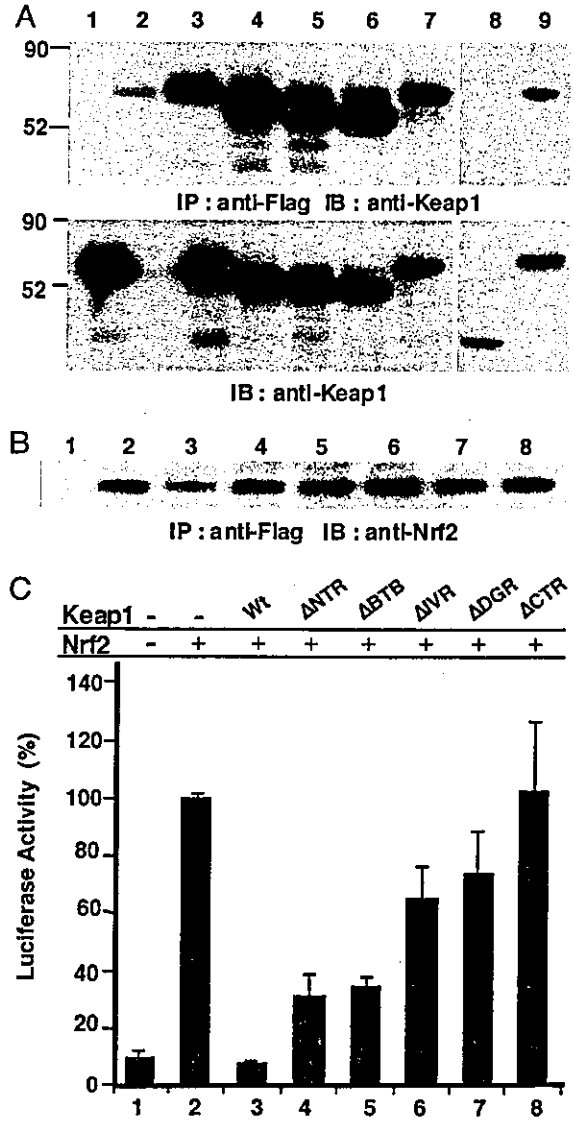

Fig. 5. IVR and CTR are both essential for Keap1 repression of Nrf2. (*A*) DGR of Keap1 directly associates with Nrf2. Whole-cell extracts prepared from 293T cells cotransfected with expression plasmids of various Keap1 deletion mutants (2 μg) and Flag-tagged Nrf2 (2 μg) were subjected to immunoprecipitation (IP). Immunoprecipitates obtained by anti-Flag antibody were subjected to immunoblot analysis (IB) with anti-Keap1 antibodies (*Upper*). The expression level of Keap1 deletion mutants was verified by immunoblot analysis (*Lower*). Analysis of cell lysates cotransfected with Nrf2 and wild-type Keap1 (lanes 3 and 9) as well as cell lysates cotransfected with Nrf2 and Keap1 ΔNTR (lane 4), ΔBTB (lane 5), ΔIVR (lane 6), ΔCTR (lane 7), or ΔDGR (lane 8) mutants are shown. Lane 1 is loaded with cell extract expressing only Keap1, and lane 2 is loaded with Nrf2 only. Anti-Keap1 CTR antibody was used in lanes 1–7, and anti-Keap1 NTR antibody was used for lanes 8 and 9. (*B*) Expression level of Nrf2 in immunoprecipitates was monitored by immunoblot analysis with anti-Nrf2 antibody. Analysis of cell lysates cotransfected with Nrf2 and wild-type Keap1 (lane 3) as well as cell lysates cotransfected with Nrf2 and Keap1 ΔNTR (lane 4), ΔBTB (lane 5), ΔIVR (lane 6), ΔCTR (lane 7), or ΔDGR (lane 8) mutants are shown. Lane 1 is loaded with cell extract expressing only Keap1, and lane 2 is loaded with Nrf2 only. (*C*) Three domains (DGR, CTR, and IVR) are crucial for the Keap1 activity. Expression plasmids of Nrf2 (90 ng) and various Keap1 deletion mutants (shown in the figure; 10 ng) were transfected into NIH 3T3 cells (2×10^4) along with a reporter plasmid, pNQO1-ARE (50 ng). Assays were performed in triplicate.

DGR and CTR Are both Indispensable to Suppress the Transactivation Activity of Nrf2. We then examined the ability of various Keap1 mutants to repress the transactivation activity of Nrf2 (Fig. 5*C*). Plasmids expressing Keap1 deletion mutants were cotransfected with plasmids expressing Nrf2 into NIH 3T3 cells along with the reporter plasmid (pNQO1-ARE) containing a single Nrf2-binding site. The luciferase activity attained by transfection of Nrf2 alone was set to 100% and used to normalize the relative activity in the presence of Keap1 mutants. Immunoblot analysis verified similar expression levels of each mutant protein (data not shown). Whereas Nrf2 activated the reporter gene expression >10-fold over the basal expression, simultaneous expression of Keap1 almost completely abolished this activation (compare lanes 1–3 in Fig. 5*C*). Transfection with ΔNTR and ΔBTB also markedly repressed the Nrf2 activity (Fig. 5*C*, lanes 4 and 5).

In contrast, deletion of the DGR and CTR from Keap1 almost abolished Keap1 activity in repressing transactivation of Nrf2 (Fig. 5*C*, lanes 7 and 8). Because ΔDGR and ΔCTR could not entrap Neh2-GFP in the cytoplasm (Fig. 4, ΔDGR and ΔCTR), these data suggest that both DGR and CTR are indispensable for Keap1 activity. Interestingly, deletion of IVR also affects the repressor activity of Keap1 (Fig. 5*C*, lane 6). This was an unexpected observation, because IVR does not interact directly with Nrf2 or actin (Figs. 2*B* and 5*A*). Four cysteine residues in IVR were recently shown to be highly reactive with electrophiles (16), and it was proposed that some of them act as sensors for electrophilic stimuli that regulate the association of Keap1 and Nrf2. The present result further supports our hypothesis that the cysteine residues in IVR are essential for Keap1 to repress the transactivation activity of Nrf2 (16).

Discussion

We investigated in this study how a cytoplasmic protein Keap1 regulates Nrf2 activity. We found that Keap1 binds to the actin cytoskeleton and traps Nrf2, thereby preventing the nuclear translocation of this transcription factor. Whereas several Kelch-related proteins are known to colocalize with actin filaments, the physiological significance of the actin binding has not been well characterized (11). This study therefore provides the first convincing evidence that the direct interaction between Keap1 and the actin cytoskeleton contributes to the regulatory activity of Keap1. The present analyses further indicated that the DGR domain of Keap1 interacts primarily and directly with Nrf2, and the CTR and IVR domains also contribute to the ability of Keap1 to retain Nrf2 in the cytoplasm. Structure–function analyses of the Keap1–Nrf2 system provide plausible molecular understanding of how Keap1 functions as a sensor for inducing this signal pathway.

Keap1 colocalizes with the actin cytoskeleton and is abundantly distributed in the perinuclear region of the cytoplasm. This localization profile of Keap1 suggests three biological roles for Keap1. First, the perinuclear localization may allow Keap1 to entrap effectively Nrf2 protein synthesized *de novo* as it migrates into the nucleus. Second, because phase 1 enzymes that initially metabolize xenobiotics are usually localized on the cytoplasmic surface of the endoplasmic reticulum (23), Keap1 has easy access to the highly reactive phase 1 products by selecting actin filaments as a scaffold. Third, recently we and other groups found that Nrf2 is degraded rapidly and efficiently with the 26S proteasome under unstressed conditions (24–27). Because the proteasome is also known to colocalize with the actin filaments and intermediate filaments (28), we envisage that Keap1 may transfer the newly synthesized Nrf2 to the proteasome localized nearby, resulting in the rapid turnover of Nrf2.

CTR consists of 26 amino acid residues, and the primary structure is not well conserved among the other Kelch-related β-propeller proteins. CTR has one reactive cysteine (Cys-613), which binds dexamethasone mesylate (16). These results suggest a unique function of Keap1 CTR among Kelch family proteins. In the structure–function analysis of Keap1, CTR was shown to be essential for Keap1 repression of Nrf2. However, deletion of

CTR did not affect Keap1 interaction with Nrf2 in the immunoprecipitation analysis (Fig. 5*A*). One plausible explanation for this discrepancy is that CTR may act indirectly to modulate DGR activity. In contrast to the present results, it was recently reported that the presence of either DGR or CTR is sufficient for Keap1 to retain Nrf2 (29). In our experiments, however, the ΔDGR mutant possessing CTR could not repress Nrf2 activity at all, indicating that DGR is absolutely required for the Keap1 retention of Nrf2 in the cytoplasm. Zhang and Hannink (30) recently reported that 15 amino acid residues from C terminus of Keap1 are not required for the Keap1 activity, whereas in our experiments, ΔCTR (26-aa deletion) could not repress Nrf2 activity, indicating that CTR is required for the Keap1 activity.

Zipper and Mulcahy recently reported that Keap1 forms a homodimeric complex through the BTB domain (9). Keap1 dimerization was suggested to be an important step for sequestration of Nrf2 in the cytoplasm and the Ser-104 residue in the BTB domain appeared to be critical for Keap1 self-association. In contrast, we found that ΔBTB-Keap1 effectively repressed Nrf2 transactivation activity (Fig. 5*C*, lane 5). Thus, deletion of the BTB domain did not impair Keap1 activity in our transfection analysis. We surmise that this discrepancy may be due to differences in the experimental conditions. Whereas the BTB domain is not the direct binding interface, it is possible that this domain may modulate the function of the DGR domain, as is the case for CTR and IVR domains.

Transcriptional regulation through the actin cytoskeleton seems to be unique to the Keap1–Nrf2 system. In this regard, it is noteworthy that Cubitus interruptus (Ci) of *Drosophila*, which is a transcription factor under the Hedgehog signal pathway (31), may have some similarity to the Keap1–Nrf2 system. In the absence of ligand Hedgehog, Ci is tethered to microtubules through forming a complex with Fused, Cos2, and Su(fu) proteins. On Hedgehog binding to the receptor Patched, an inhibitor protein Smoothened is released and it liberates Ci from microtubules. The microtubule association seems to be essential for Ci, because Slimb associated with microtubules modifies Ci to a transcriptional repressor through cleavage. Because Keap1-mediated tethering of Nrf2 to the actin cytoskeleton provokes degradation of Nrf2 (26, 27), the actin cytoskeleton seems to provide a scaffold for protein modification and degradation in the Keap1–Nrf2 system.

We thank Drs. Paul Talalay, Pamela Talalay, Makoto Kobayashi, Albena Dinkova-Kostova, Hozumi Motohashi, Ken Itoh, and Thomas W. Kensler for help and discussion. This work was supported in part by grants from Japan Science and Technology Agency–Exploratory Research for Advanced Technology (to M.Y.), the Ministry of Education, Sciences, Sports, and Technology (to A.K. and M.Y.), and the Ministry of Health, Labor, and Welfare (to M.Y.).

1. Nguyen, T., Sherratt, P. J. & Pickett, C. B. (2003) *Annu. Rev. Pharmacol. Toxicol.* **43**, 233–260.
2. Moi, P., Chan, K., Asunis, L, Cao, A. & Kan, Y. W. (1994) *Proc. Natl. Acad. Sci. USA* **91**, 9926–9930.
3. Itoh, K., Igarashi, K., Hayashi, N., Nishizawa, M. & Yamamoto, M. (1995) *Mol. Cell. Biol.* **15**, 4184–4193.
4. Itoh, K., Chiba, T., Takahashi, S., Ishii, T., Igarashi, K., Katoh, Y., Oyake, T., Hayashi, N., Satoh, K., Hatayama, I., *et al.* (1997) *Biochem. Biophys. Res. Commun.* **236**, 313–322.
5. Ishii, T., Itoh, K., Takahashi, S., Sato, H., Yanagawa, T., Katoh, Y., Bannai, S. & Yamamoto, M. (2000) *J. Biol. Chem.* **275**, 16023–16029.
6. Motohashi, H., O'Connor, T., Katsuoka, F., Engel, J. D. & Yamamoto, M. (2002) *Gene* **294**, 1–12.
7. Itoh, K., Wakabayashi, N., Katoh, Y., Ishii, T., Igarashi, K., Engel, J. D. & Yamamoto, M. (1999) *Genes Dev.* **13**, 76–86.
8. Xue, F. & Cooley, L. (1993) *Cell* **72**, 681–693.
9. Zipper, L. M. & Mulcahy, R. T. (2002) *J. Biol. Chem.* **277**, 36544–36552.
10. Ito, N., Phillips, S. E., Yadav, K. D. & Knowles, P. F. (1994) *J. Mol. Biol.* **238**, 794–814.
11. Adams, J., Kelso, R. & Cooley, L. (2000) *Trends Cell Biol.* **10**, 17–24.
12. Kim, L F., Mohammadi, E. & Huang, R. C. (1999) *Gene* **228**, 73–83.
13. Hayes, J. D., Chanas, S. A., Henderson, C. J., McMahon, M., Sun, C., Moffat, G. J., Wolf, C. R. & Yamamoto, M. (2000) *Biochem. Soc. Trans.* **28**, 33–41.
14. Wakabayashi, N., Itoh, K., Wakabayashi, J., Motohashi, H., Noda, S., Takahashi, S., Imakado, S., Kotsuji, T., Otsuka, F., Roop, D. R., *et al.* (2003) *Nat. Genet.* **35**, 238–245.
15. Dinkova-Kostova, A. T., Massiah, M. A., Bozak, R. E., Hicks, R. J. & Talalay, P. (2001) *Proc. Natl. Acad. Sci. USA* **98**, 3404–3409.
16. Dinkova-Kostova, A. T., Holtzclaw, W. D., Cole, R. N., Itoh, K., Wakabayashi, N., Katoh, Y., Yamamoto, M. & Talalay, P. (2002) *Proc. Natl. Acad. Sci. USA* **99**, 11908–11913.
17. Niwa, H., Yamamura, K. & Miyazaki, J. (1991) *Gene* **108**, 193–200.
18. Bubb, M. R., Spector, I., Bershadsky, A. D. & Korn, E. D. (1995) *J. Biol. Chem.* **270**, 3463–3466.
19. Jordan, A., Hadfield, J., Lawrence, N. J. & McGown, A. T. (1998) *Med. Res. Rev.* **18**, 259–296.
20. Theodoropoulos, P. A., Gravanis, A., Tsapara, A., Margioris, A. N., Papadogiorgaki, E., Galanopoulos, V. & Stournaras, C. (1994) *Biochem. Pharmacol.* **47**, 1875–1881.
21. Kang, K. W., Lee, S. J., Park, J. W. & Kim, S. G. (2002) *Mol. Pharmacol.* **62**, 1001–1010.
22. Soltysik-Espanola, M., Rogers, R. A., Jiang, S., Kim, T. A., Gaedigk, R., White, R. A., Avraham, H. & Avraham, S. (1999) *Mol. Biol. Cell* **10**, 2361–2375.
23. Guengerich, F. P. (1990) *Crit. Rev. Biochem. Mol. Biol.* **25**, 97–153.
24. Nguyen, T., Sherratt, P. J., Huang, H. C., Yang, C. S. & Pickett, C. B. (2003) *J. Biol. Chem.* **278**, 4536–4541.
25. Stewart, D., Killeen, E., Naquin, R., Alam, S. & Alam, J. (2002) *J. Biol. Chem.* **18**, 2396–2402.
26. McMahon, M., Itoh, K., Yamamoto, M. & Hayes, J. D. (2003) *J. Biol. Chem.* **278**, 21592–21600.
27. Itoh, K., Wakabayashi, N., Katoh, Y., Ishii, T., O'Connor, T. & Yamamoto, M. (2003) *Genes Cells* **8**, 379–391.
28. Arcangeletti, C., Sutterlin, R., Aebi, U., De Conto, F., Missorini, S., Chezzi, C. & Scherrer, K. (1997) *J. Struct. Biol.* **119**, 35–58.
29. Dhakshinamoorthy, S. & Jaiswal, A. K. (2001) *Oncogene* **20**, 3906–3917.
30. Zhang, D. D. & Hannik, M. (2003) *Mol. Cell. Biol.* **23**, 8137–8151.
31. Aza-Blanc, P. & Kornberg, T. B. (1999) *Trends Genet.* **5**, 458–462.

Small Maf proteins serve as transcriptional cofactors for keratinocyte differentiation in the Keap1–Nrf2 regulatory pathway

Hozumi Motohashi*, Fumiki Katsuoka*, James Douglas Engel†, and Masayuki Yamamoto*‡§

*Institute of Basic Medical Sciences and Center for Tsukuba Advanced Research Alliance and ‡Exploratory Research for Advanced Technology, Environmental Response Project, University of Tsukuba, Tsukuba 305-8577, Japan; and †Department of Cell and Developmental Biology and Center for Organogenesis, University of Michigan, Ann Arbor, MI 48109-0616

Edited by Mark T. Groudine, Fred Hutchinson Cancer Research Center, Seattle, WA, and approved March 9, 2004 (received for review September 12, 2003)

The small Maf proteins, MafF, MafG, and MafK, possess a leucine zipper (Zip) domain that is required for homodimer or heterodimer complex formation with other bZip transcription factors. In this study we sought to determine the identity of the specific constituent that collaboratively interacts with Nrf2 to bind to the Maf recognition element *in vivo*. Studies *in vitro* suggested that Nrf2 forms heterodimers with small Maf proteins and then bind to Maf recognition elements, but the bona fide partner molecules supporting Nrf2 activity *in vivo* have not been definitively identified. Nrf2 activity is usually suppressed by a cytoplasmic repressor, Keap1, so disruption of the *keap1* gene causes constitutive activation of Nrf2. Nrf2 hyperactivity results in hyperproliferation of keratinocytes in the esophagus and forestomach leading to perinatal lethality. However, simultaneous disruption of *nrf2* rescued *keap1*-null mice from the lethality. We exploited this system to investigate whether small Mafs are required for Nrf2 function. We generated *keap1* and small *maf* compound mutant mice and examined whether keratinocyte abnormalities persisted in these animals. The data show that loss of *mafG* and *mafF* in the *keap1*-null mice reversed the lethal keratinocyte dysfunction and rescued the *keap1*-null mutant mice from perinatal lethality. This rescue phenotype of *mafG::mafF::keap1* triple compound mutant mice phenocopies that of the *nrf2::keap1* compound mutant mice, indicating that the small Maf proteins MafG and MafF must functionally cooperate with Nrf2 *in vivo*.

A central issue in deciphering the regulatory mechanisms mediated by the activity of transcription factors is how to best evaluate the *in vivo* contribution of each protein–protein and transcription factor–DNA interaction that is defined *in vitro*. Transcription factors that interact with Maf recognition elements (MARE) possess a basic region-leucine zipper (bZip) domain and form dimers that can be characterized by a potentially enormous combinatorial array (1). *In vitro* analysis has shown that MARE binding complexes consist mainly of: (*i*) four large Maf or three small Maf protein homodimers; (*ii*) heterodimer complexes containing a small Maf with any of six different Cap-N-Collar (CNC) family proteins; and (*iii*) homo- or heterodimers composed of Jun and Fos family members (2–4). To elucidate MARE-dependent gene regulatory mechanisms, we need to identify the major participants among all these possible interacting molecules in an *in vivo* context.

The small Maf proteins, MARE-binding components that were originally identified as cellular homologs of the v-*maf* oncogene (4–6), dimerize among themselves and with other bZip factors, usually CNC or Bach family proteins (7–11). The small Maf family consists of only three members, MafF, MafG, and MafK, but to date, other than their differential tissue distribution (12), no functional differences among the three have been revealed. The CNC family includes NF-E2 p45, Nrf1, Nrf2, and Nrf3 (7, 9, 13, 14), and Bach family proteins are closely related to CNC members (10). While small Maf proteins lack any recognizable transcriptional effector domains, CNC and Bach families possess transactivation or -repression domains unique to each molecule. Through heterodimerization, the small Maf protein confers DNA-binding specificity to its CNC or Bach partner molecule on the MARE sequence, and enables these heterodimers to execute differential activating or repressing activities as dictated by their encoded functional domains.

The Maf proteins recognize either a T-MARE, containing a TPA responsive element (TRE), or a C-MARE, containing a cAMP responsive element (CRE) as a core sequence. In these MAREs, the core consensus motifs are flanked on each side by three conserved residues "TGC" and "GCA" at the 5′ and 3′ ends, respectively. The DNA binding specificity of Maf proteins is achieved through their inherent recognition of these flanking sequences, whereas the other bZip factors, such as Nrf2 and Fos, recognize primarily the TRE or CRE core sequences. A previous NMR study revealed that the structural basis for the unique "GC" requirement of Maf proteins for DNA binding is caused by the presence of an extended homology region, which is conserved only within the Maf family (15).

Germ-line mutagenesis of the *nrf2* gene revealed that Nrf2 is an essential component for antioxidant and detoxification enzyme gene expression (16). Nrf2 transcriptional activity is controlled by an interaction between Nrf2 and the cytoplasmic regulatory protein Keap1 (17). When cells are exposed to electrophiles or reactive oxygen species (ROS), Nrf2 is released from Keap1 cytoplasmic capture, leading to its translocation to the nucleus, where Nrf2 activates transcription of target genes. The marked susceptibility of *nrf2*-null mutant mice to the toxicity of electrophiles and ROS demonstrates the importance of Nrf2 for protection against oxidative stress (18–20). We therefore generated *keap1*-null mutant mice, anticipating that Nrf2 might be constitutively activated in the absence of Keap1, thereby conferring resistance to electrophilic stress. To our surprise, the *keap1*-null mutant mice died before weaning due to a hyperkeratotic proliferative disorder (21). The cornified layers of esophageal and forestomach stratified squamous epithelia were abnormally thickened, thereby obstructing the lumen. We found that this epithelial phenotype was completely rescued by the additional disruption of *nrf2*, indicating that the *keap1*-null phenotype reflects a gain of Nrf2 function.

There has been some uncertainty regarding the identity of the heterodimeric partner molecule of Nrf2 *in vivo*. *In vitro* studies have shown strong DNA binding activity of Nrf2-small Maf heterodimers (16, 22, 23), which supported our contention that this complex actually functions as a major transcriptional activator *in vivo*. However, although strong transactivation activity was observed when Nrf2 was overexpressed in culture cells, addition of small Maf to the transfection reaction led to reporter

This paper was submitted directly (Track II) to the PNAS office.

Abbreviations: MARE, Maf recognition element; CNC, Cap-N-Collar.

§To whom correspondence should be addressed. E-mail: masi@tara.tsukuba.ac.jp.

gene repression in most cases (22, 24–26). Hence, the question we sought to answer was whether or not the Nrf2/small Maf heterodimer is the functionally active species that acts at MAREs *in vivo*.

Alternative candidates for heterodimeric partner molecule of Nrf2 have been suggested. For example, c-Jun and ATF-4 were reported to cooperate with Nrf2 for gene activation *in transfecto* (27, 28). However, because disruption of *c-jun* or *atf-4* does not cause a defect similar to that observed in *nrf2*-null mutant animals (29–31), it remains to be clarified whether these factors can heterodimerize with Nrf2 to transduce transcriptional responses from MAREs *in vivo*. Similarly, a functional contribution of small Maf proteins to Nrf2 activity has not been well documented in small *maf* mutant mice.

Because disruption of the *keap1* gene causes severe dysfunction of keratinocytes that leads to perinatal lethality, but simultaneous disruption of *nrf2* rescued *keap1*-null mice from the lethality, we exploited this compound knockout–rescue approach to investigate whether small Mafs actually function cooperatively with Nrf2 and activate transcription *in vivo*. To this end, we generated *keap1*::small *maf* compound knockout mutant mice and examined whether a reduction in small Maf activity, as does the loss of Nrf2, mitigates the *keap1*-null phenotype. We show here that simultaneous disruption of the *mafG* and *mafF* genes rescued the *keap1*-null pups from perinatal lethality, allowing them to survive to adulthood. Thus, the small *maf*::*keap1* mutant mice phenocopy the rescue phenotype of *nrf2*::*keap1* compound mutant mice, demonstrating that the small Maf proteins cooperatively function with Nrf2 *in vivo*.

Materials and Methods

Generation of the Small *maf*::*keap1* Compound Mutant Mice. Germline mutagenesis of the murine *mafF*, *mafG*, *mafK*, *nrf2*, and *keap1* genes has been described (12, 16, 21, 32). All of the mice examined in this study were of mixed genetic background with contributions from 129Sv/J, C57BL/6J, and ICR. Genotypes were determined by PCR. The body weight of each mouse was measured weekly. More than three independent animals of each genotype were first weighed on postnatal day 7, and then followed to the 6th week.

Histological Analysis. Two-day-old pups, 10- to 12-day-old pups, and 4-month-old mice were killed, and the forestomach was dissected. Samples for staining with hematoxylin and eosin were fixed in 3.7% formaldehyde overnight and then embedded in paraffin. LacZ staining was performed as described (33). Samples for immunostaining with antibodies against Nrf2 or keratin 6 were fixed in PBS containing 1% formaldehyde, 0.2% glutaraldehyde, and 0.02% Nonidet P-40 for 30 min, embedded in OCT compound (Tissue-tek, Sakura Finetechnical, Chuo-ku, Tokyo), followed by frozen sectioning with a cryostat. The antibody against Nrf2 (C-20, Santa Cruz Biotechnology) was used at a 1:400 dilution; immunoreactivity was visualized with an avidin-biotin-peroxidase kit (Vector Laboratories). The antibody recognizing keratin 6 (PRB-169P, Covance, Princeton) was used at a 1:500 dilution.

Quantitative Real-Time PCR. Total RNA was extracted from the forestomach of 10- to 12-day-old pups using ISOGEN (Nippon Gene, Toyama, Japan). Random cDNA was synthesized from the isolated RNAs, and real-time PCR (ABI PRISM 7700) was performed as described (12) with minor modifications. To measure the copy number of each mRNA, plasmids harboring each cDNA were used as standards. Oligonucleotide sequences used for detecting MafF mRNA are available upon request.

RNA Blot Analysis. Total RNA was prepared as described above. Total RNA (2 μg per lane) was used for electrophoresis, followed by hybridization to radiolabeled probes. The keratin 6 probe was generated by PCR (primer sequences are available upon request). The PCR product was cloned, sequenced, and used as a probe for detecting the transcripts of both keratin 6 genes (i.e., keratin 6a and keratin 6b).

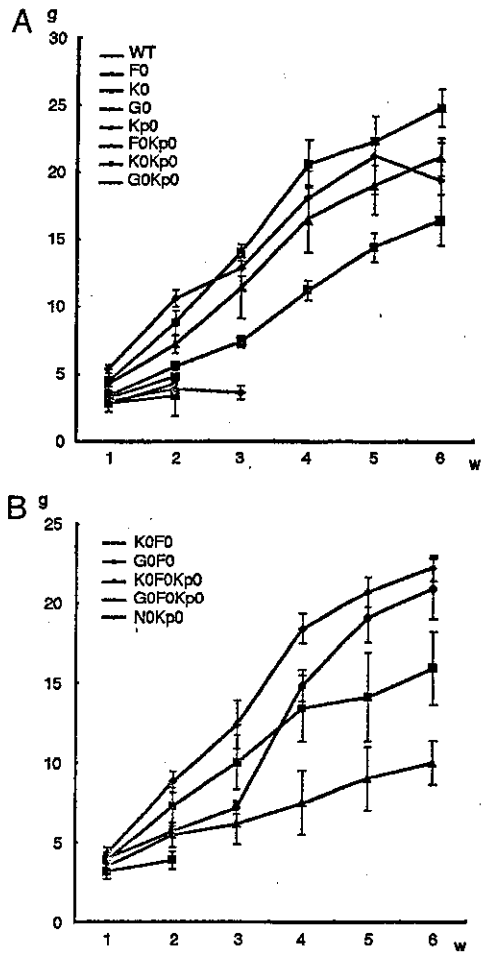

Fig. 1. Small *maf*::*keap1* compound mutant mice survive beyond weaning. (*A*) Body weight change for mice bearing single small *maf* gene disruptions in the *keap1*-null background. Deletion of either *mafK* or *mafF* did not extend the lifespan of *keap1*-null mutant pups. When *mafG* alone was disrupted in addition to *keap1*, pups survived one week longer. (*B*) Body weight change for mice with compound small *maf* gene disruptions in the *keap1*-null mutant background. Simultaneous deletion of *mafG* and *mafF* rescued the lethality of *keap1*-null mutant pups. The body weight of *nrf2*::*keap1* mice was examined as a control. WT indicates wild-type; F0, *mafF*−/−; K0, *mafK*−/−; G0, *mafG*−/−; N0, nrf2−/−; Kp0, *keap1*−/−.

Results

Simultaneous Loss of *mafG* and *mafF* Rescues *keap1*-Null Mutant Postnatal Lethality. To ask whether a reduction in small Maf activity mitigates the *keap1*-null phenotype, we crossed small *maf* mutant mice with *keap1* mutants to generate compound mutant animals. When *mafK* or *mafF* was deleted in addition to *keap1*, no pups survived beyond weaning (Fig. 1*A*; precisely the same phenotype as in the *keap1* mutants), but the life span of *mafG*::*keap1* compound mutant mice was approximately one week longer than mice bearing only the *keap1* mutant alleles (Fig. 1*A*, G0Kp0 mice), suggesting that the *mafG* contribution to keratinocytic homeostasis is greater than that of either MafK or MafF.

Because the results of small *maf* compound mutant analyses indicate that three small Mafs are capable of compensating for one another (34), we next further reduced the number of active small *maf* alleles in the *keap1*-null background. Whereas mice bearing disruptions in all three small *maf* genes might have been preferred

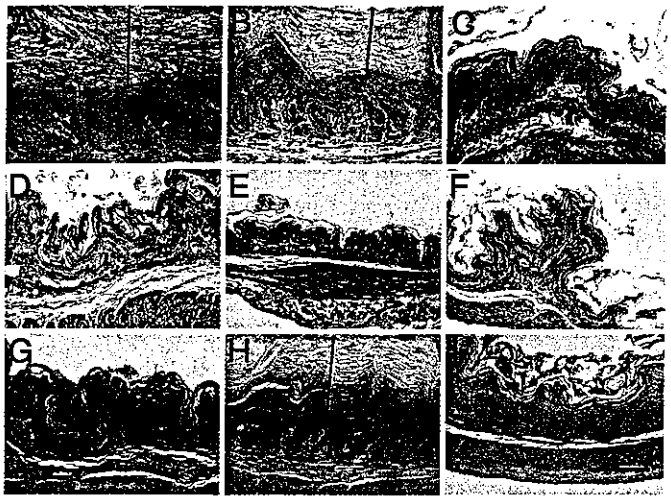

Fig. 2. Histological examination of forestomach. Hematoxylin/eosin staining of 10-day-old forestomach thin sections from Kp0 (*A*), F0Kp0 (*B*), G0F0Kp0 (*C*), WT (*D*), F0 (*E*), and G0F0 (*F*) pups are shown. Sections of the forestomach from 4-month-old mice of WT (*G*), G0F0Kp0 (*H*), and N0Kp0 (*I*) genotypes are also presented. Double-ended arrows indicate the cornified layer. (Scale bar, 150 μm.)

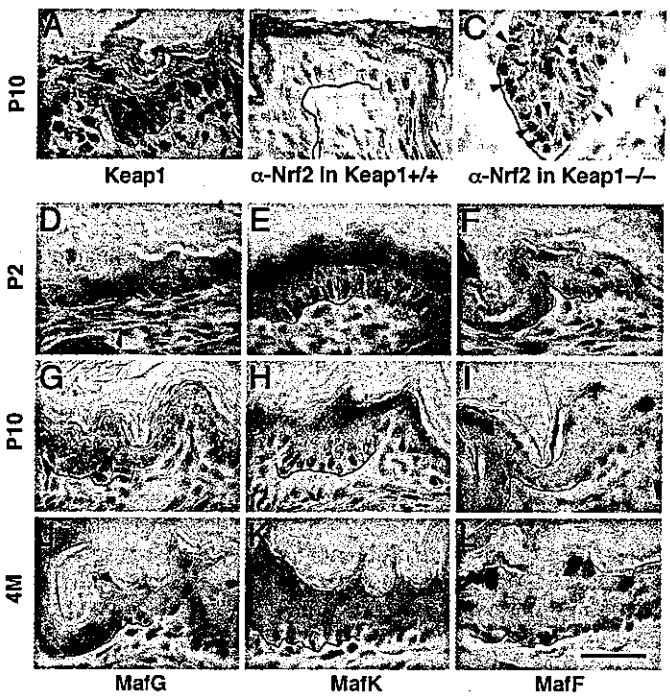

Fig. 3. Expression profiles of Keap1, Nrf2, and small Mafs in the forestomach. (*A*) LacZ staining of squamous cell epithelia in the forestomach of *keap1* heterozygous mutant mice. Blue staining is observed in LacZ-expressing cells. (*B* and *C*) Immunohistochemistry with anti-Nrf2 antibody. Brown punctate staining, indicated by arrowheads, is observed within nuclei of *keap1*-null mutant cells (*C*), whereas no staining develops in wild-type keratinocytes (*B*). Nonspecific staining is observed in the cornified epithelial layers. (*D–L*) LacZ staining of squamous cell epithelia of the forestomach in sections prepared from *mafG* (*D*, *G*, and *J*), *mafK* (*E*, *H*, and *K*), and *mafF* (*F*, *I*, and *L*) heterozygous mutant mice. Samples were prepared from 2-day-old (*D–F*), 10-day-old (*G–I*), or 4-month-old (*J–L*) mice. The green lines indicate the position of basement membranes. (Scale bar, 30 μm throughout.)

for this analysis, mice lacking all small Mafs die by midgestation (unpublished observations). Similarly, *mafG::mafK* compound mutant mice expire before weaning (34). We therefore examined instead two genotypes that were healthy and fertile (i.e., *mafG::mafF* and *mafF::mafK* compound mutants) in combination with the mutant *keap1*-null alleles (Fig. 1*B*). Whereas disruption of both *mafK* and *mafF* did not rescue *keap1* mutant from lethality (K0F0Kp0 mice), when the *mafG* and *mafF* genes were simultaneously deleted in the *keap1*-null background the mice survived for more than four months (G0F0Kp0 mice in Fig. 1*B*).

Because we previously found that the simultaneous deletion of *nrf2* with *keap1* genes almost completely reversed the *keap1*-null mutant phenotype (21), we compared the body weight gain of G0F0Kp0 mice with that of *nrf2::keap1* compound mutant mice (N0Kp0 mice) to evaluate the efficiency of the rescue by simultaneous *mafG* and *mafF* deletion. Whereas N0Kp0 mice showed a similar body weight gain to that of wild-type mice, G0F0Kp0 mice were much smaller than both of these at 6 weeks after birth (Fig. 1). G0F0Kp0 mice were also smaller than G0F0 mice (G0F0Kp0 vs. G0F0 in Fig. 1*B*), indicating that the effect of the Keap1 deficiency is only partially overcome in G0F0Kp0 mice. These results demonstrate that Keap1 deficiency provokes constitutive activation of Nrf2 and the growth retardation of mice, but this deleterious effect of Keap1 loss can be partially circumvented by the simultaneous loss of MafG and MafF.

Improvement of Hyperkeratosis in Forestomach and Esophagus of *mafG::mafF::keap1* Triple Mutant Mice. We next performed histological analysis of the forestomach and esophagus of the rescued triple compound mutant (i.e., G0F0Kp0) animals at 10 days after birth (Fig. 2 and data not shown). Heavily thickened cornified layers, convoluted basal layers, and thickened spinous and granular layers were observed in the forestomach of *keap1*-null mutant and F0Kp0 mice (Fig. 2 *A* and *B*), whereas G0F0Kp0 mice displayed a normal stratified squamous epithelium (Fig. 2*C*), similar to the control samples (Fig. 2 *D–F*).

Because the body weight difference was apparent between G0F0Kp0 and N0Kp0 mice at 6 weeks of age, we hypothesized that the constitutive elevation of Nrf2 activity in the *keap1*-null background was only partially overcome in G0F0Kp0 mice and that the rescue of the *keap1*-null phenotype might be incomplete. In support of this contention, we found that the forestomach epidermal layers of G0F0Kp0 mice were hyperkeratotic, whereas those of the N0Kp0 forestomach were almost indistinguishable from wild type (Fig. 2 *G–I*). We envisage that in contrast to *keap1*-null mutant mice, thickening of the cornified epithelial layers develop more gradually in the G0F0Kp0 forestomach as a consequence of residual elevated Nrf2 activity.

Keratinocyte Abnormality Is Involved in the Hyperkeratosis Observed in *keap1*-Null Mice. To determine whether diminished Keap1 expression in keratinocytes might lead to the observed hyperkeratosis, we examined *keap1* gene expression in the stratified squamous epithelium by monitoring the expression of the *LacZ* gene that was inserted into the *keap1* locus when the gene was disrupted (21). β-Galactosidase activity was observed primarily in keratinocytes of whole layers of stratified squamous epithelium, from the immature cells in basal layers to the granular layers composed of more differentiated cells (Fig. 3*A*). The green lines in Fig. 3 define the position of the basement membrane. These data indicate that Keap1 is predominantly expressed in keratinocytes, regardless of differentiation stage.

We next examined Nrf2 activation in the unstimulated, but pathologically expanded, forestomach epithelium of *keap1*-null mutant mice by examining the epithelial cells for nuclear accumulation of Nrf2 protein. Keap1 sequesters Nrf2 in the cytoplasm and prevents it from traversing into the nucleus (17). Recent reports showed that Nrf2 is constantly degraded by the proteasome when cells are not stimulated (35–38), thus keeping Nrf2 concentration

low, whereas Nrf2 is translocated into the nucleus and is stabilized upon exposure to electrophilic reagents or oxidative stress. We performed immunohistochemical examination of the keratinocytes of *keap1*-null animals using an antibody that specifically recognizes Nrf2. As expected, intranuclear foci were observed in the forestomach epithelium of the *keap1*-null mutant mice (Fig. 3*C*, arrowheads); also as anticipated, no Nrf2 was detected in comparable cells of a wild-type littermate (Fig. 3*B*), consistent with the notion that proteasome-mediated turnover leads to rapid degradation of Nrf2 in the unstimulated cytoplasm. These results thus demonstrate that the control processes mediated by Nrf2 and Keap1 are actually extant in forestomach keratinocytes. The results also suggest that gene dysregulation within keratinocytes is involved in the hyperkeratosis observed in *keap1*-null mutant mice.

Small Maf Proteins Are Expressed in Forestomach Keratinocytes. The rescue experiments described above suggest that diminished small Maf activity is required for correction of the *keap1*-induced keratinocytic abnormality, and that the small Mafs must therefore act in the same genetic pathway as Nrf2 to execute the transcriptional program in keratinocyte differentiation (Fig. 1). However, none of the small *maf* mutant phenotypes described to date include keratinocytic abnormalities; no report has emerged demonstrating any functional contribution of small Mafs to keratinocyte biology.

Therefore, we examined the expression of the three small *maf* genes in the forestomach epithelium by monitoring LacZ activity in the small *maf* mutants, because each of the small *maf* knockouts was generated by simultaneous insertion of a *LacZ* gene. While we inserted the normal *LacZ* gene into the *mafK* and *mafG* loci, the *mafF* insertion contained lacZ linked to a nuclear localization signal (NLS). At 10 days after birth, β-galactosidase activity was observed throughout the layers of stratified squamous epithelium in the *mafG* mutant mice (Fig. 3*G*). Expression of *mafK* is weaker in the basal cells and stronger in more differentiated cells of the spinous and granular layers (Fig. 3*H*). Interestingly, *mafF* is expressed almost exclusively in the most differentiated granular layer cells (Fig. 3*I*). β-Galactosidase activity was localized in the cytoplasm of keratinocytes in *mafK* and *mafG* mutant mice, which gave rise to both diffuse and punctate staining (Fig. 3 *G* for *mafG* and *H* for *mafK*), but the activity was exclusively nuclear in keratinocytes of *mafF* mutant mice (Fig. 3*I*). These expression patterns were reproducible when 2-day-old pups and 4-month-old adult mice were analyzed for each small *maf* gene (Fig. 3 *D–F* and *J–L*). β-Galactosidase staining was especially intense in the granular layer of *mafK* mutant mice, regardless of developmental stage (Fig. 3 *E*, *H*, and *K*). The abundance of all three small *maf* gene mRNAs was almost constant from neonatal stages to adulthood, when monitored by quantitative real-time PCR (data not shown). Thus, all three small Maf proteins are expressed in the forestomach squamous epithelium, and the expression patterns are indeed overlapping with those of Nrf2 and Keap1.

MafG Is a Major Small Maf Protein Species in Keratinocytes. To determine whether there were any correlations between the mRNA abundance and the functional contribution of each small *maf* gene, the copy numbers of each small Maf mRNA expressed in the forestomach at 10 days after birth were quantified by quantitative real-time PCR, and MafG mRNA was found to be the most abundant small Maf (Fig. 4). The observed abundant MafG expression in the forestomach shows very good agreement with the data in the small *maf* gene knockout–rescue experiments (Fig. 1), which suggest that MafG makes the largest contribution to normal keratinocyte function among the three small Maf proteins. We conclude that *mafG* and *mafF* disruption attained a significant enough reduction in the total amount of small Maf protein that there was no longer sufficient Maf activity present in cells to effectively execute Nrf2 function.

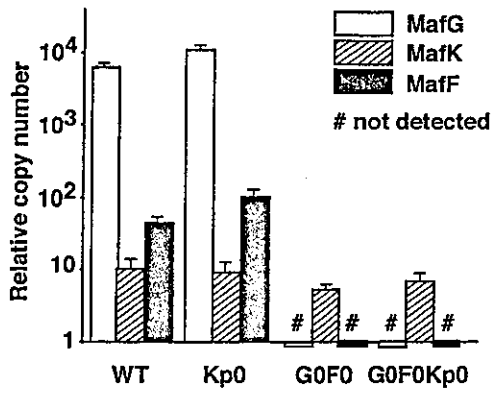

Fig. 4. Quantification of small Maf mRNA abundance in forestomach. cDNA was synthesized from total RNA prepared from WT, Kp0, G0F0, and G0F0Kp0 forestomach at 10 days after birth. MafG, MafK, and MafF mRNA levels were quantified by quantitative real-time PCR using a plasmid containing each cDNA as the abundance standard.

Increased Keratin 6 Expression Returns to Normal Levels in the Forestomach of *mafG::mafF::keap1* Triple Mutant (Rescued) Mice. Keratin 6 is strongly induced in the *keap1*-null mutant esophagus, and it has been suggested to be a direct Nrf2 target gene in keratinocytes. The expression of keratin 6 was dramatically induced in the forestomach epithelium of the *keap1*-null mice, judging from the strong immunohistochemical anti-keratin 6 staining (Fig. 5 *A* and *B*). Consistent with the distribution of constitutively activated Nrf2 in the *keap1* mutant mice (see Fig. 3*C*), keratin 6 was induced in all keratinocyte layers (Fig. 5*B*). To investigate whether increased keratin 6 expression in the *keap1*-null mutant forestomach is caused by constitutive activation of Nrf2, we analyzed keratin 6 expression in N0Kp0 compound mutant mice. Keratin 6 mRNA was abundant in the *keap1* mutant (Fig. 5*D*, lanes 3 and 4), but was scarcely detectable in either the wild-type or N0Kp0 animals (Fig. 5*D*, lanes 1, 2, 11, and 12), thus confirming the Nrf2-dependency of *keratin 6* gene activation.

We then examined the expression of keratin 6 in the rescued G0F0Kp0 mice. Application of anti–keratin 6 antibody did not generate a signal in the forestomach epithelial layers of G0F0Kp0 mice (Fig. 5*C*), and, as in the N0Kp0 mutant, the G0F0Kp0 mutant forestomach expressed the same low levels of keratin 6 mRNA as wild-type mice (Fig. 5*D*, lanes 9 and 10). These results thus demonstrate that the small Maf proteins are required for Nrf2-dependent transcriptional activation of the *keratin 6* gene.

Although the double deletion of *mafF* and *mafG* rescued the lethality of *keap1* null mutants, *mafF* deletion alone did not affect the lifespan of *keap1*-null pups (F0Kp0 in Fig. 1), and ablation of *mafG* extended their lifespan by only one week (G0Kp0 in Fig. 1). These results suggested that the rescue efficiency of each compound mutant mouse inversely correlates with the remaining small Maf activity; Kp0 mice possess full activity, and small Maf abundance in keratinocytes appears to be reduced in the order: F0Kp0 > G0Kp0 > G0F0Kp0. Hence we hypothesized that the expression of keratin 6 mRNA would be higher in the order: Kp0 > F0Kp0 > G0Kp0 > G0F0Kp0. In the hope of detecting graded expression of keratin 6 mRNA, we further examined G0Kp0 and F0Kp0 mice.

Contrary to our expectation, keratin 6 mRNA was hardly detectable except in the Kp0 and F0Kp0 mutants (Fig. 5*D*, lanes 1, 2, and 7–12). Considering the similarity in low-level expression of keratin 6 in G0Kp0 and G0F0Kp0 mice, some additional factors may be involved in the large difference in weight gain and viability between the mice of two genotypes. A second unexpected result was that keratin 6 is more abundant in *mafF::keap1* double mutant than *keap1* single mutant forestomach (Fig. 5*D*, lanes 3–6). Interestingly, when small *maf* expression levels were examined, *mafG* was found

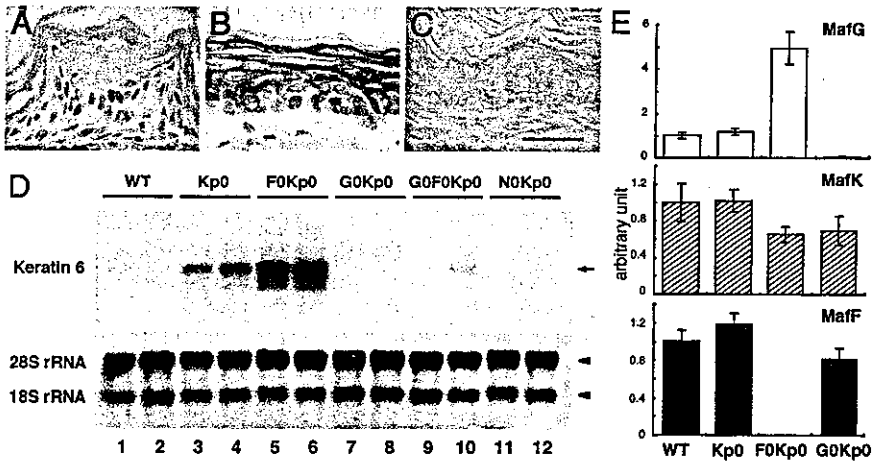

Fig. 5. Expression of keratin 6 as a marker of Nrf2-mediated transcriptional activity. (*A–C*) Immunohistochemistry with anti-keratin 6 antibody. Keratin 6 is highly expressed in *keap1*-null keratinocytes in the forestomach (*B*), whereas no signals were observed in the wild-type (*A*) or rescued G0F0Kp0 (*C*) mice. (Scale bar, 30 μm in *A–C*.) (*D*) Keratin 6 expression levels were examined by RNA blot analysis. Total RNA prepared from wild-type (lanes 1 and 2), Kp0 (lanes 3 and 4), F0Kp0 (lanes 5 and 6), G0Kp0 (lanes 7 and 8), G0F0Kp0 (lanes 9 and 10), and N0Kp0 (lanes 11 and 12) mice forestomachs are shown. The arrow and arrowheads indicate keratin 6 mRNA and ribosomal RNAs (18S and 28S), respectively. (*E*) Relative expression levels of the three small *maf* genes in the forestomach of wild-type, Kp0, F0Kp0, and G0Kp0 at 10 days after birth (compared with the levels in wild-type mice).

to be highly induced in *mafF*::*keap1* double mutant forestomach (Fig. 5*E*).

Discussion

It has been postulated that the small Maf proteins function as major heterodimeric partner molecules of Nrf2 based principally on *in vitro* DNA binding evidence. Heterodimer formation between Nrf2 and the small Mafs was detected by using bacterially expressed proteins or *in vitro* translated proteins (14, 16, 22, 24, 28, 39, 40), and substantial efforts have been made to document endogenous Nrf2-small Maf complexes capable of interacting with MAREs (23, 25, 41, 42). Although these studies have shown Nrf2-small Maf heterodimer formation, the question remained whether Nrf2-small Maf heterodimer actually functions as a transcription activator or whether Nrf2 might require an alternative partner to activate MARE-dependent target genes, because in many transfection assays cooperative activation of Nrf2 and small Mafs was not observed (22, 24–26). Hence the aim of this study was to test the contention that small Mafs cooperate with Nrf2 to activate transcription in an *in vivo* experimental system.

To address this issue, we generated *keap1* and small *maf* compound gene knockout mice and asked whether the loss of one or two small *maf* genes in concert with the *keap1* gene affected the lethal phenotype of Keap1-null mutant mice caused by the hyperactivity of Nrf2. We found that loss of *mafG* and *mafF* indeed rescued the *keap1*-null mutant mice from perinatal lethality. Because the rescue phenotype of *mafG*::*mafF*::*keap1* triple compound mutant mice is similar to that of the *nrf2*::*keap1* compound mutant mice, we conclude that small Maf proteins are indispensable components for Nrf2-dependent transcription *in vivo*. These results further support the contention that Nrf2-small Maf heterodimers serve as indispensable transcriptional regulators of keratinocytic gene expression.

We suggested previously that *loricrin* and *keratin 6* are potential Nrf2 target genes in keratinocytes (21). There is one potential MARE in *loricrin* "CCA*TGGTGACATAGC*TTGAA", and two MAREs in *keratin 6*, "TGA*TGGTGAGC*TT*GCA*GAGT," and "GTG*TGGTGAGGGGGCA*CACA," ≈40 bp and 300 bp 5′ to the TATA boxes, respectively (nucleotides corresponding to a typical T-MARE, "TGCTGA$^{G}/_{C}$TCAGCA," are italicized). These sequences correspond closely to the consensus sequence of antioxidant responsive elements (ARE), well characterized Nrf2 target sites that exist in the regulatory regions of phase 2 detoxifying enzyme genes and oxidative stress-inducible genes (43). In this study, we monitored *keratin 6* as a parameter for measuring Nrf2 transcriptional activity, because the expression profile of *keratin 6* corresponds closely to the distribution of Keap1-Nrf2 system in forestomach (see Fig. 5 *A* and *B*). Importantly, the increase in expression of *keratin 6* observed in the *keap1* mutant background returned to normal levels by simultaneous deletion of either *nrf2* or deletion of both *mafG* and *mafF*.

When we examined *mafF*::*keap1* compound mutant forestomach in the hope of detecting an intermediate expression level of keratin 6, an unexpected result emerged, in that the level of keratin 6 mRNA in F0Kp0 pups was higher than in the Kp0 pups (Fig. 5*D*). One intriguing explanation for this result can be drawn from the unanticipated induction of *mafG* expression in the F0Kp0 forestomach (Fig. 5*E*). The regulatory mechanisms controlling *mafG* levels in the forestomach seem to be sensitive to the total amount of small Mafs, whereas those controlling *mafK* and *mafF* do not. MafG mRNA expression might be elevated because of compensatory mechanisms whose nature is unknown at present, but may involve autoregulation of a subset of the small Mafs. Consequently, more small Maf proteins are produced in the F0Kp0 forestomach, ending in higher expression of keratin 6 mRNA than in Kp0 mice. This result, although surprising, nonetheless further supports the contention that small Maf cooperatively activates Nrf2-dependent transcription *in vivo*.

Given the complexity of MARE-dependent gene regulation, germ-line mutagenesis and loss of function studies of each gene have proven to be a powerful approach to glean insight into the function of the molecules that interact with this site *in vivo*. Because small Maf proteins are capable of heterodimerizing with many bZip factors, including the CNC and Bach proteins, diminished small Maf abundance should be reflected by a functional defect in the activity of these multiple partner molecules. Megakaryocytic defects result as a consequence of defective p45 function or to a small Maf deficiency (32, 44–46). Similarly, aberrant constitutive induction of *heme oxygenase-1* can be attributed to a functional defect of Bach1 with insufficient small Maf partner molecules (47, 48). The other phenotypes observed in compound *small maf* mutant mice are red cell membrane abnormalities and a profound neurological disorder (34, 48), neither of which have been encountered in the analysis of Nrf2-deficient mice. This observation likely indicates